Protist, Vol. 169, 158–179, xx 2018
http://www.elsevier.de/protis
Published online date 21 February 2018

Protist

ORIGINAL PAPER

Phylogeny and Morphology of New Diplonemids from Japan

Daria Tashyreva[a,2], Galina Prokopchuk[a,2], Akinori Yabuki[b,2], Binnypreet Kaur[a,c,2], Drahomíra Faktorová[a,c], Jan Votýpka[a,d], Chiho Kusaka[b], Katsunori Fujikura[b], Takashi Shiratori[e], Ken-Ichiro Ishida[f], Aleš Horák[a,c], and Julius Lukeš[a,c,1]

[a]Institute of Parasitology, Biology Centre, Czech Academy of Sciences, České Budějovice (Budweis), Czech Republic
[b]Department of Marine Diversity, Japan Agency for Marine-Earth Science and Technology, Yokosuka, Japan
[c]Faculty of Science, University of South Bohemia, České Budějovice (Budweis), Czech Republic
[d]Faculty of Sciences, Charles University, Prague, Czech Republic
[e]Graduate School of Life and Environmental Sciences
[f]Faculty of Life and Environmental Sciences, University of Tsukuba, Tsukuba, Japan

Submitted June 28, 2017; Accepted February 5, 2018
Monitoring Editor: Alastair Simpson

Diplonemids were recently found to be the most species-rich group of marine planktonic protists. Based on phylogenetic analysis of 18S rRNA gene sequences and morphological observations, we report the description of new members of the genus *Rhynchopus* – *R. humris* sp. n. and *R. serpens* sp. n., and the establishment of two new genera – *Lacrimia* gen. n. and *Sulcionema* gen. n., represented by *L. lanifica* sp. n. and *S. specki* sp. n., respectively. In addition, we describe the organism formerly designated as *Diplonema* sp. 2 (ATCC 50224) as *Flectonema neradi* gen. n., sp. n. The newly described diplonemids share a common set of traits. Cells are sac-like but variable in shape and size, highly metabolic, and surrounded by a naked cell membrane, which is supported by a tightly packed corset of microtubules. They carry a single highly reticulated peripheral mitochondrion containing a large amount of mitochondrial DNA, with lamellar cristae. The cytopharyngeal complex and flagellar pocket are contiguous and have separate openings. Two parallel flagella are inserted sub-apically into a pronounced flagellar pocket. *Rhynchopus* species have their flagella concealed in trophic stages and fully developed in swimming stages, while they permanently protrude in all other known diplonemid species.

Key words: *Diplonema*; ultrastructure; phylogeny; Euglenozoa; description; flagellates.

Introduction

Diplonemids are colorless heterotrophic, predominantly marine protists, equipped with two flagella. They belong to Euglenozoa and are thus related to ecologically important euglenids and econom-

[1]Corresponding author; fax +420 387775416
[2]These authors contributed equally to this work.
e-mail jula@paru.cas.cz (J. Lukeš).

https://doi.org/10.1016/j.protis.2018.02.001

ically and medically relevant kinetoplastids (Adl et al. 2012; Maslov et al. 1999; Moreira et al. 2001). For a long time, diplonemids were considered a small and rare group of flagellates with only three genera and less than a dozen species formally described (Massana 2011; Simpson 1997; Vickerman 2000; von der Heyden et al. 2004). However, they emerged from obscurity thanks to molecular analysis of hundreds of planktonic samples collected across the globe by several research expeditions (de Vargas et al. 2015; Lara et al. 2009). The recent Tara Oceans 18S rRNA-based metabarcoding survey revealed remarkable diversity and abundance of marine diplonemids: with over 45,000 operational taxonomic units (OTUs), they qualify as the most species-rich marine planktonic eukaryotes (David and Archibald 2016; Flegontova et al. 2016). Furthermore, diplonemids show cosmopolitan distribution with different lineages being abundant and often dominant in most ocean niches, from shallow littoral sediments (Larsen and Patterson 1990) to deep aphotic pelagic waters (de Vargas et al. 2015; Flegontova et al. 2016; Gawryluk et al. 2016; Lara et al. 2009), hydrothermal vents (López-García et al. 2007), and down to poorly studied abyssopelagic zones (Eloe et al. 2011; Scheckenbach et al. 2010).

According to 18S rRNA-based phylogeny, diplonemids represent a monophyletic group which can be subdivided into four robustly supported lineages: (i) the so-called classic diplonemids, hereafter referred to as Diplonemidae, consisting of the genera *Diplonema* and *Rhynchopus*; (ii) a small planktonic clade containing the genus *Hemistasia*; (iii) a deep-sea pelagic diplonemids (DSPD) clade I and (iv) DSPD clade II (Flegontova et al. 2016). DSPD I diplonemids were recently formally described as Eupelagonemidae (Okamoto et al., submitted; this work). While this phylogeny shows a clear support for diplonemid monophyly, the relationships between these major lineages are unclear. Most of the species richness is apparently confined within the hyperdiverse Eupelagonemidae clade which, together with DSPD II, was until recently known exclusively from environmental sequences, and we still lack any cultured representative (Flegontova et al. 2016; Lara et al. 2009; Lukeš et al. 2015). However, the single-cell approach provided a first glance at morphological diversity and genomic characteristics of members of the Eupelagonemidae, although it was stressed that poor quality of genomic assemblies and possible contamination necessitates establishment of stable cultures (Gawryluk et al. 2016).

Despite their abundance, huge diversity and consequently importance in marine food webs, very little is known about the behavior as well as molecular, morphological and biochemical traits of diplonemids (David and Archibald 2016). Indeed, there are only four species altogether for which both morphological observations and sequence data, albeit limited, is available: two members of the genus *Diplonema* – *D. papillatum* (Maslov et al. 1999; Porter 1973) and *D. ambulator* (Busse and Preisfeld 2002; Montegut-Felkner and Triemer 1996; Triemer and Ott 1990; Triemer 1992), and a single species for each of the genera *Rhynchopus* and *Hemistasia*, namely *Rhynchopus euleeides* (von der Heyden et al. 2004; Roy et al. 2007) and *Hemistasia phaeocysticola* (Elbrächter et al. 1996; Yabuki and Tame 2015), respectively. However, virtually all molecular studies, such as the analysis of mitochondrial RNA editing and *trans*-splicing, were performed solely on *D. papillatum* (Kiethega et al. 2013; Marande et al. 2005; Marande and Burger 2007; Moreira et al. 2016; Vlcek et al. 2011;). Otherwise, a few other species known from early morphological studies, namely *Diplonema breviciliata* (Griessmann 1913), *D. nigricans* (Schuster et al. 1968), *D. metabolicum* (Larsen and Patterson 1990), *Rhynchopus amitus* (Skuja 1948), and *R. coscinodiscivorus* (Schnepf 1994), lack any molecular data and are unavailable in culture. Moreover, several putative species have been classified according to their 18S RNA gene sequences and are available at the American Type Culture Collection (ATCC) but lack proper morphological description (von der Heyden et al. 2004).

Diplonemids belonging to the genera *Diplonema* and *Rhynchopus*, or Diplonemidae, were only marginally present in the global metabarcoding dataset (Flegontova et al. 2016). Still, the number of putative diplonemid OTUs revealed by environmental molecular barcodes available on public databases greatly exceeds the currently recognized number of species. Despite their newly discovered abundance and diversity, to the best of our knowledge, no new classic diplonemid species have recently been described. Therefore, we attempted to establish axenic cultures by manual picking of diplonemid-like cells from samples collected in surface waters around Japan. Based on phylogenetic analysis of nearly full-size 18S rRNA gene sequences and morphological observations using electron and light microscopy, we report the description of four new diplonemid species and two new genera. In addition to this, we create a novel

genus to accommodate a protist previously referred to as *Diplonema* sp. 2 (ATCC50224).

Results

Molecular Phylogeny

We have created three datasets differing by the composition of the outgroup and analyzed them using maximum likelihood and Bayesian inference (see Methods for details). Both methods applied on the dataset K (diplonemids rooted with kinetoplastids only) yielded a highly congruent topology, differing mainly by branching support of some clades (Fig. 1). The monophyly of Diplonemidae, including new members described in this study (see Taxonomic summary), is highly supported. While the internal relationships in Diplonemidae cannot be clearly resolved, there are three main robustly supported clades: (i) a clade containing *D. papillatum*, *D. ambulator* and *Diplonema* sp. ATCC50232, as well as several environmental sequences; (ii) a clade comprising of *Rhynchopus euleeides* (ATCC50226), *Rhynchopus* sp. (ATCC50229) and a few sequences from uncultured isolates, as well as two *Rhynchopus* spp. introduced into culture during of this study and formally described as new species *R. humris* sp. n. and *R. serpens* sp. n. (see below). The last main group identified within Diplonemidae is an abundant assemblage of environmental sequences (iii) described here for the first time, which is represented by an isolate introduced into culture and formally described as a new genus and species *Lacrimia lanifica* gen. n., sp. n. (see below). *Diplonema* sp. 2 (ATCC50224) is formally described here as *Flectonema neradi* gen. n., sp. n. (see below) branches outside of these three main clades along with one environmental sequence (i.e., EU635682), although this position is not highly supported. Finally, YPF1618, formally described in this study as *Sulcionema specki* gen. n., sp. n. (see below), is shown to be the most basal lineage of all classic diplonemids, including the new members.

We have tested the alternative positions of *F. neradi* and *S. specki* using the AU-test. The constrained ML tree in which *F. neradi* and *Diplonema* species form a clade is not rejected (*p*-value: 0.121) and the other constrained ML tree showing the monophyly of *F. neradi*, *S. specki* and *Diplonema* species is not rejected either (*p*-value: 0.077).

Analyses of auxiliary datasets with outgroup expanded by the addition of euglenids (E) or euglenids and heterolobosean (H) yielded very similar topologies to that of dataset K. Composition of individual 'genus-level' clades remained the same, however, the branching order mainly within the *Diplonema* and *Rhychopus* clade slightly differed in nodes with low support in dataset E. In dataset H, *Rhynchopus* branched with the new clade containing *Lacrimia lanifica* to the exclusion of *Diplonema* and the overall support for both datasets decreased, most likely due to the more diverged outgroup sequences and lower number of characters available for analysis (Supplementary Material Fig. SA1 A, B).

Light Microscopy

In order to characterize five strains that in phylogenetic analyses formed novel species, we proceeded to their morphological characterization. Differences on the light microscopy level, while not substantial, were sufficient for their distinction (Table A1A).

Rhynchopus humris

Cells cultivated axenically in a fresh, nutrient-rich medium (= trophic cells) are uniform in size and shape. The cells are of elongated to elliptical shape, dorsoventrally flattened, and narrowed at both ends (Fig. 2 A). The length ranges from 12.5 to 16.4 μm (14.5 ± 1.2 μm; n = 25), and the width is between 3.3 and 5.1 μm (4.2 ± 0.59 μm; n = 25). The cells carry two very short flagella buried in the flagellar pocket and thus are invisible by light microscopy. Prominent granulation is observed throughout the cytoplasm. The cells are typically attached to the flask bottom with a small fraction floating freely in the medium but gradually detach as cultures become older. The surface-attached cells move slowly by gliding and frequently change their direction (Fig. 3A). The cells are highly metabolic which is displayed as frequent twisting and contracting-extending movements (Table A1A).

When starved, cells reduce their size up to 7.2×3.2 μm, and the prominent cytoplasmic granulation disappears. *Rhynchopus humris* gradually develops large number of swimming cells with unequally long heterodynamic flagella (Fig. 2B, C), which are about twice of the body length and used for fast cell propulsion. The swimming cells slightly oscillate and move in a straight line but can abruptly stop and change the direction. One flagellum is twisted around the anterior part of the cell wobbling like a lasso, and the other flagellum waving and stretched along the body (Fig. 2C). The flagella are parallel-orientated and arise from subapical flagellar pocket. No cysts were observed in either starved or old batch cultures (Table A1B). Cell divi-

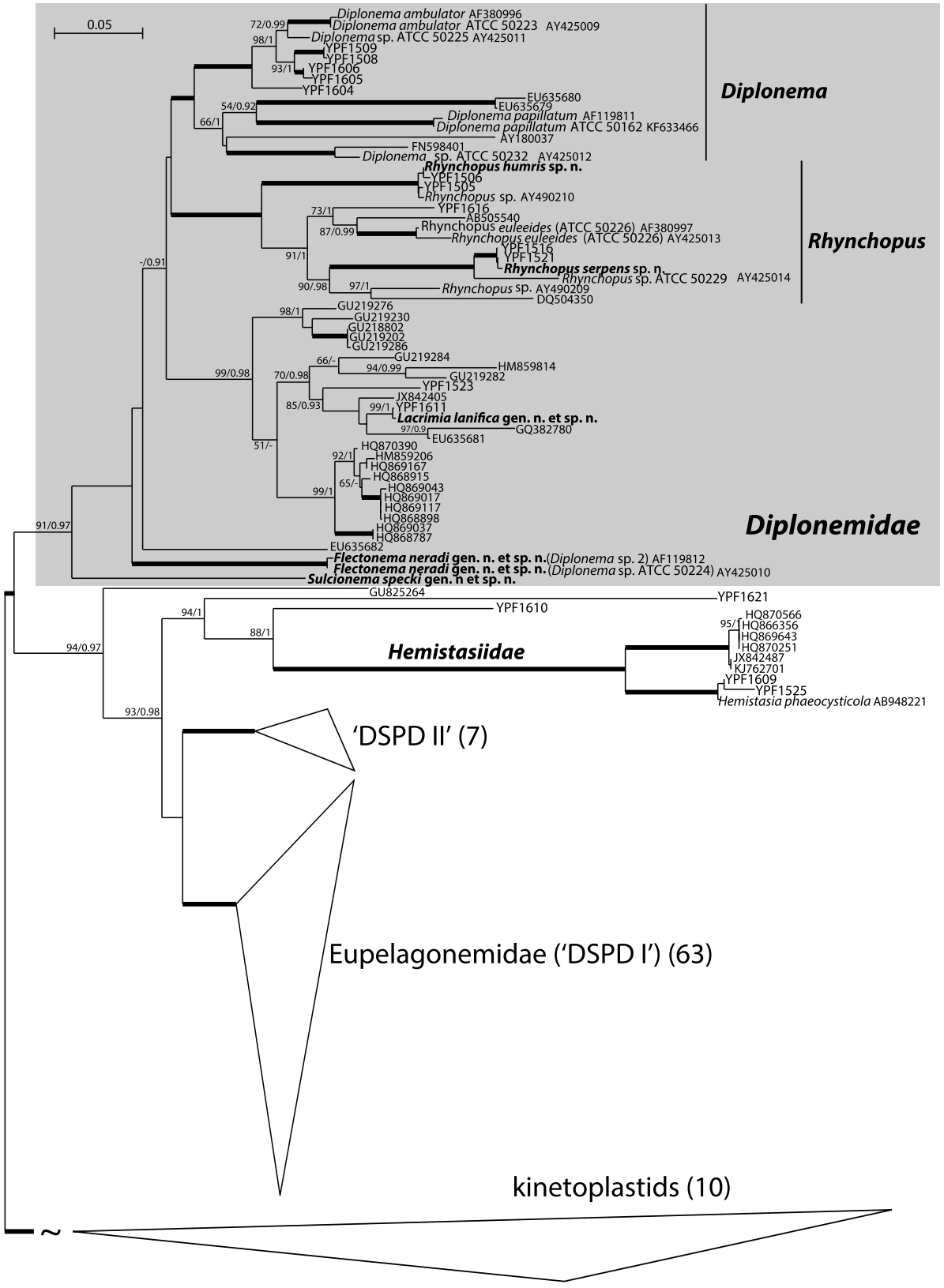

Figure 1. Maximum likelihood (ML) phylogeny of diplonemids based on 18S rRNA dataset K (kinetoplastid

sion occurs by binary fission from the anterior to posterior end, producing two equal daughter cells.

DAPI staining of the DNA reveals that in *R. humris*, the nucleus is often located proximally to the cell's periphery (Fig. 4A, B). In most cells, a network of mitochondrial DNA is located peripherally under the plasma membrane (Fig. 4A), clearly without any kinetoplast-like structure. The patchy character of mitochondrial DNA staining was often observed in *R. humris*, in both starved and non-starved cells (Fig. 4B).

Rhynchopus serpens

Cells in nutrient-rich medium (trophic cells) are consistent in morphology and have little variability in size. The cells are elongated, dorsoventrally flattened, tapered at the anterior, and rounded as well as widened at the posterior ends (Fig. 2D). They measure 21.3 to 28.7 μm (26.0 ± 1.7 μm; n = 25) in length, and 7.2 to 9 μm (8.0 ± 0.6 μm; n = 25) in width. Numerous cytoplasmic vesicles are concentrated at the posterior part of *R. serpens* cells. The short flagella stubs are concealed in the flagellar pocket and invisible under light microscopy. Cells typically attach to the flask bottom, move slowly by gliding and show frequent metabolic movements (Table A1A; Fig. 3B).

As cultures become denser, the cells progressively display greater variability in size, and often detach from the surface. Numerous cytoplasmic refractive bodies prominently present in cells of well-growing cultures diminish or completely disappear in aging cultures and in the starvation medium, indicating that they possibly serve as food reserves. The cells attain a more symmetrical shape but preserve the acute apex and eventually halve in size (13.5 × 3.7 μm). The swimming stages (Fig. 2E, F) occur less frequently than in *R. humris* cultures. The cells are symmetrical and elongated, notably dorsoventrally compressed, tapering at the cell apex. Two unequally long flagella (2 to 2.5 times of the body length) are parallel and inserted into a pronounced flagellar pocket. The swimming is slow when both *R. serpens* flagella are stretched along the body and perform waving movements (Fig. 2E; Table A1B), whereas fast propulsion occurs when the anterior flagellum forms a loop beating rapidly before the anterior end (Fig. 2F; Table A1B). Cysts are not produced. Cells divide by binary fission.

DAPI staining shows that the nucleus has a variable position within *R. serpens* cells, and reveals a network of mitochondrial DNA beneath the cell surface forming aggregates but lacking kinetoplast-like structures (Fig. 4C). Multiple attempts to stain the mitochondrion with specific dyes and immunolabelling worked only in starved *R. serpens*, in which a reticulated mitochondrion was stained with 6 μM $DiOC_6(3)$, regardless of the presence of DMSO. In non-starved cells, the signal from the mitochondrion was hindered by very bright fluorescence of cytoplasmic inclusion bodies that non-specifically took up the $DiOC_6(3)$ dye. The staining revealed that a mitochondrion, most likely single, forms a network, which occupies a substantial part of the cell's periphery (Fig. 4D). In some cases, the network seems to split into several smaller oval-shaped organelles, which remain located under the cell surface (Fig. 4E).

Lacrimia lanifica

Cells in well growing cultures are nearly isodiametric but often teardrop-shaped due to the presence of large digestive vacuoles at the posterior end, while the anterior end is narrowed (Fig. 2G). They are 10.4 to 15.3 μm long (13.1 ± 1.3 μm; n = 25) and 7.3 to 10.5 μm wide (8.7 ± 0.74 μm; n = 25). *Lacrimia lanifica* cells tend to form homogeneously suspended cultures, and invariably possess two unequally long flagella (about the body length) inserted sub-apically into a conspicuous flagellar pocket. When suspended in the medium, *L. lanifica* constantly maintains rotational movement with its two flagella (Table A1A), and is also capable of gliding along the surface by attaching to it with its longer flagellum. In culture, *L. lanifica* displays metabolic movements mostly when attached temporarily to the surface with its body or flagellum, however, these movements become frequent when the cells are trapped under a coverslip or embedded in 0.5% ultralow gelling agarose (Fig. 3C). Cell divi-

outgroup, 133 taxa, 2000 nucleotides) inferred using IQ-Tree 1.5b under the GTR model with six relaxed rate categories. Branching support (numbers at respective nodes) is represented by non-parametric bootstrapping (BS) estimated from 1000 replicates using thorough algorithm in IQ-Tree as well as by Bayesian posterior probabilities (PP) estimated in Phylobayes 4.1 (C40 + GTR model). For Bayesian inference (BI), 0.95 probability was used as a support criterion, d.t. means different topology of respective node in BI compared to ML. Bold lines represent absolute support (100 BS/1.0 PP).

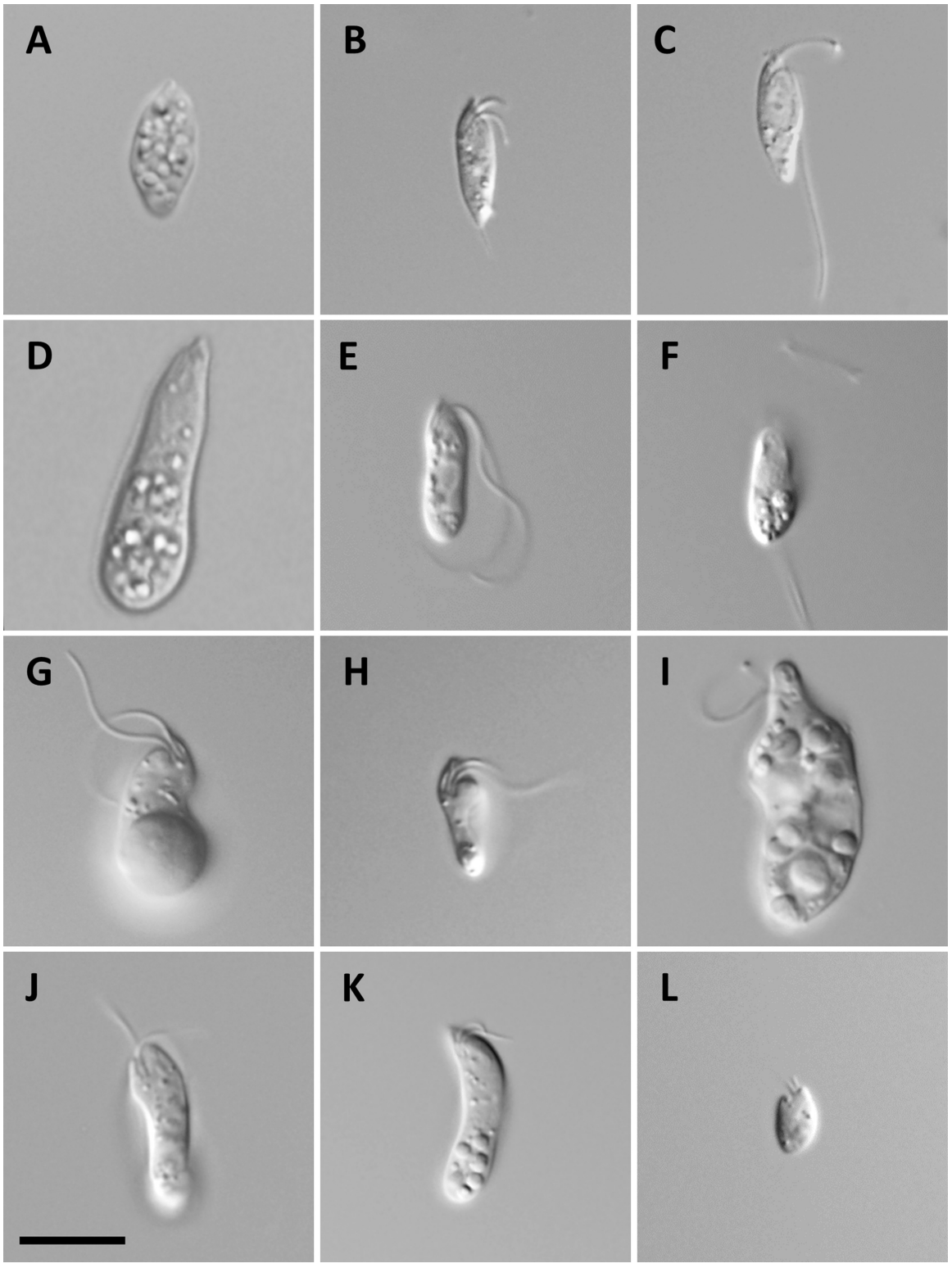

Figure 2. Differential interference contrast images of living cells. Cells of *Rhynchopus humris* (**A**), *Rhynchopus serpens* (**D**), *Lacrimia lanifica* (**G**), *Sulcionema specki* (**I**), and *Flectonema neradi* (**K**) from nutrient-rich medium. Note the absence of flagella in both *Rhynchopus* species. Cells of *R. humris* with partially (**B**) and fully developed

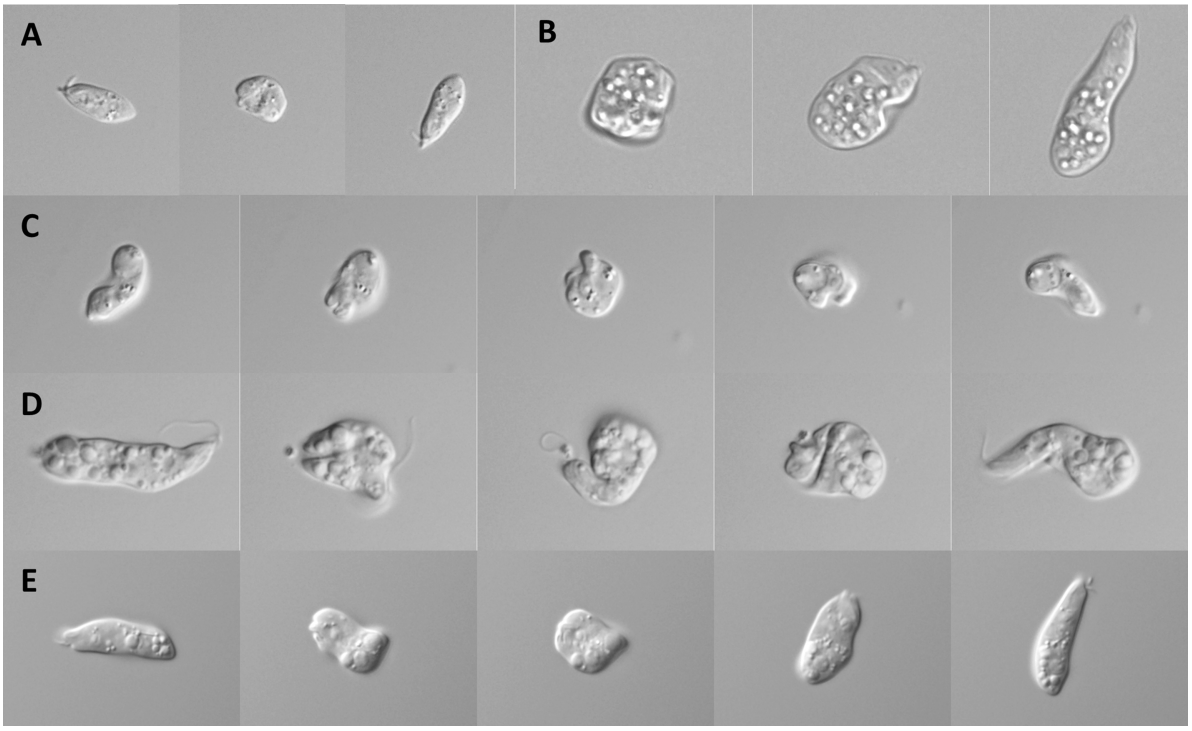

Figure 3. Differential interference contrast images of live cells. Contracting-extending and twisting metabolic movements of starved *R. humris* (**A**), *R. serpens* (**B**), starved *L. lanifica* (**C**), *S. specki* (**D**), and *F. neradi* (**E**). Scale bar is 10 μm.

sion occurs by binary fission producing two equal daughter cells, both with digestive vacuoles, or only one of the daughter cells receives the vacuole.

In aged and starved cultures, the cells become notably smaller (7.5 × 3.6 μm) and attain more elongated shape, however, the length of flagella mostly remains unchanged. The food vacuoles become small or disappear (Fig. 2H). Some of the starved *L. lanifica* cells are capable of fast swimming in a straight line through spiral oscillating movement (Table A1B). No cysts produced.

DAPI staining reveals the mitochondrial network beneath the cell's surface (Fig. 4F), and a nucleus in the anterior part of the cell. Regardless of the nutrition, the mitochondrial network sometimes splits into separate small aggregates (Fig. 4G).

Sulcionema specki

Cells are noticeably flattened with tapered, slightly crooked anterior along with rounded posterior ends, and contain conspicuous cytoplasmic granulation (Figs 2I, 3D). The cells range between 23.7 and 33.3 μm (27.6 ± 2.1 μm; n = 25) in length and 5.8 to 9.6 μm (7.4 ± 0.9 μm; n = 25) in width although smaller cells also occur, possibly as a result of recent binary fission. *Sulcionema specki* tends to form homogeneously suspended cultures, and possesses two equal to subequal flagella, which are about a third of the body length and inserted subapically in a flagellar pocket. The flagella support only erratic 'floundering'-like movement without cell propulsion. Cells are highly metabolic, which is displayed as frequent radical contortions, twisting, and contraction-extension reminiscent of amoeboid movement (Table A1A; Fig. 3D).

The cell shape, dimensions, and cytoplasmic granulation vary considerably depending on the age of cultures and content of nutrients in the medium. With the age of cultures and after transfer to the starvation medium, the *S. specki* cells begin to display great morphological variability, ranging

(**C**) flagella, *R. serpens* with partially (**E**) and fully developed (**F**) flagella following starvation treatment. *L. lanifica* (**H**), *S. specki* (**J**), and *F. neradi* (**L**) after 7-day starvation. Note the decrease of cytoplasmic granulation in all species. Scale bar is 10 μm.

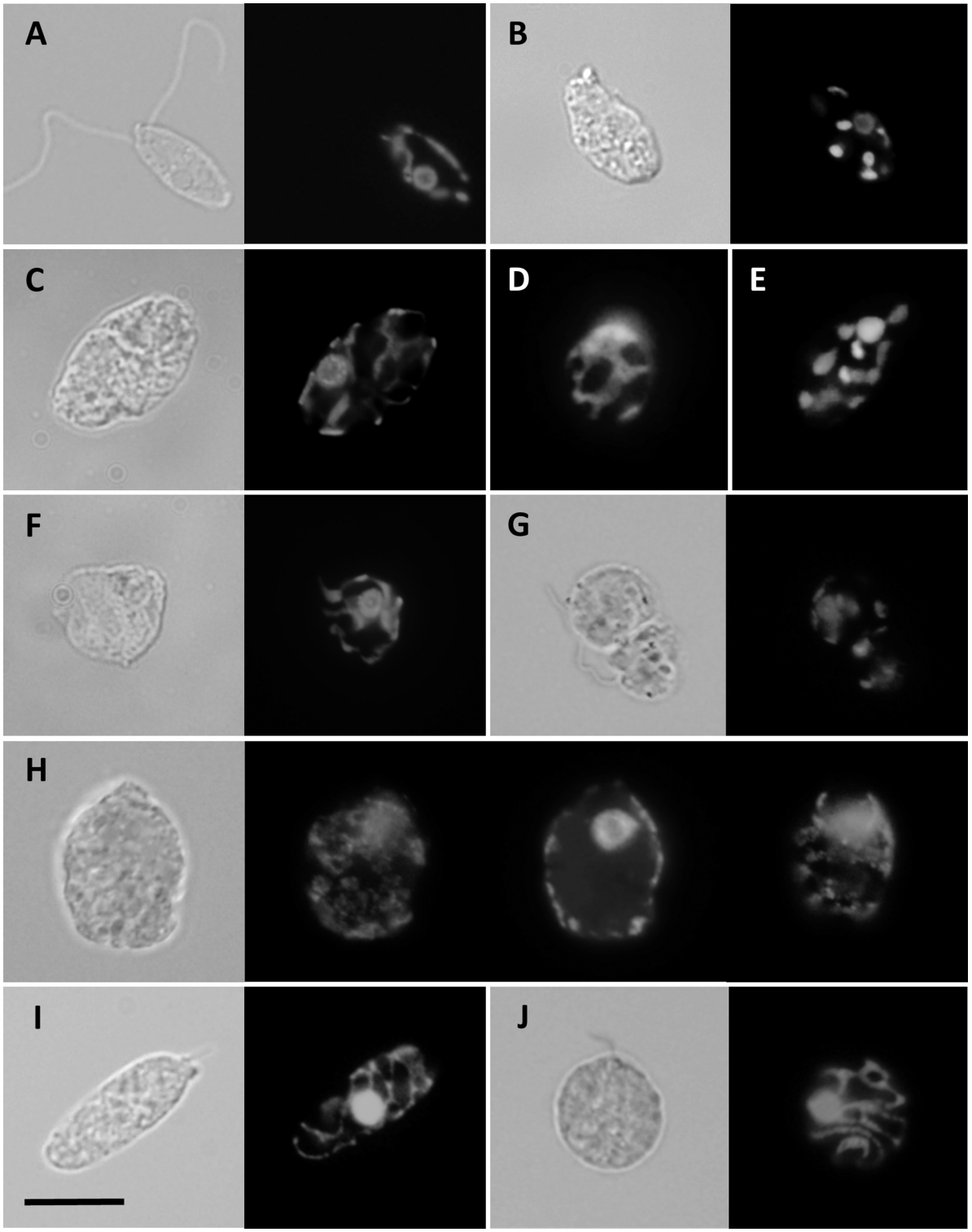

Figure 4. Light and fluorescence micrographs of fixed DAPI-stained cells (**A-C, F-J**). Swimming (**A**) and trophic (**B**) *R. humris* cells with peripheral nuclei; trophic *R. serpens* cell (**C**); non-starved *L. lanifica* cells (**F, J**); a series of images focused through non-starved *S. specki* cell with the nucleus in the anterior part (**H**); non-starved *F. neradi* cells (**I, J**). Note that mitochondrial DNA forms a network in all species but is split into isolated aggregates in *R. humris* (**B**) and *L. lanifica* (**G**). Fluorescence microscopy of starved live *R. serpens* cells stained with $DiOC_6(3)$ reveals extensive mitochondrial network (**D**) or possibly fragmented mitochondria (**E**). Scale bar is 10 μm.

from short oval to considerably elongated cells, with both ends either rounded or constricted (Fig. 2J). The smallest cell measured only 16.3 × 5 μm, with flagella the same length as in the nutrient-rich medium. The conspicuous cytoplasmic inclusions greatly reduce in size or completely disappear. Although the cells become noticeably smaller, no fast swimming cells were observed even after 10-day incubation in the starvation medium, and the character of their movement remained unchanged (Table A1B). No cysts were observed.

Mitochondrial DNA, stained with DAPI, appears as numerous agglomerates occupying nearly the entire cell's subsurface (Fig. 4H). The nucleus is mostly located at the posterior part of cells (Fig. 4H).

Flectonema neradi

The cells in nutrient-rich medium show little variability in size and shape. They are dorsoventrally flattened, thin and crooked as well as constricted at both ends, which gives a crescent-like shape, with granulation in the posterior region (Fig. 2K). The length ranges from 15.9 to 20.9 μm (18.3 ± 1.45 μm; n = 25), and the width is between 3.5 and 5.8 μm (4.0 ± 0.6 μm; n = 25). *Flectonema neradi* cells are mostly attached to the flask surface, display pronounced metaboly (Fig. 3E), move slowly by gliding, and frequently change their direction. The species invariably possesses two equal flagella emerging sub-apically, which are about a fifth of the body length. Cells often temporarily attach to the flask surface with one of their short flagella and rotate around their anterior end (Table A1A). Cell division occurs by binary fission from the anterior to posterior end, producing two equal daughter cells.

No fast swimming stages or cysts can be observed in old batch cultures and after the starvation treatment. Starved cells are short and mostly rounded, or have constricted posterior ends (Fig. 2L). The dimensions of cells reduces (down to 6.3 × 3.1 μm) along with the length of their flagella. The cytoplasmic inclusions are small or absent (Table A1B).

Mitochondrial DNA is organized as a fine network anastomosing peripherally under the plasma membrane (Fig. 4I, J). The nucleus can occupy various positions within cells.

Electron Microscopy

Scanning EM revealed relatively slight differences in general morphology between the examined isolates (Fig. 5). *Rhynchopus humris* (Fig. 5A, F), *R. serpens* (Fig. 5B, G), *S. specki* (Fig. 5D, I) exhibit long cylindrical or rounded cells, as is the case of *L. lanifica* (Fig. 5C, H), which has the cells tapered anteriorly with subapically inserted flagella. A cylindrical cell is also a characteristic of *F. neradi* (Fig. 5E), whose distinctive feature is that the opening of the flagellar pocket is extended into a curved groove, giving the anterior end a twirl-like appearance (Fig. 5J). The cell surface of all described species is generally smooth, though some pimples can occasionally be found in the anterior part of *R. serpens* (Fig. 5B). Invariably, the opening to the feeding apparatus contiguous with the flagellar pocket is located at the anterior end. The opening is characterized by a prominent collar-like cytostome with an apical papillum (Fig. 5F-J).

Comparison of ultrastructural features observed by TEM revealed similarity in the common organelles and structures in all species examined (Fig. 6). Immediately beneath the cell membrane lies a single-layer corset of peripheral, evenly spaced microtubules interlinked by fine lateral bridges (Fig. 7A-E). These microtubules seem to enfold the cell in a helical pattern. The corset is absent along the zone of flagellar attachment (Fig. 8A-E), and forms a perpendicular junction in the flagellar pocket region (Fig. 7A-E). Tubules of endoplasmic reticulum (ER) are often seen under the microtubular corset (Figs 6, 7). Beneath the microtubules is a dense mitochondrial network anastomosing around the periphery of the cell (Fig. 7F-J). The mitochondria contain variable but overall exceptionally large lamellar cristae, with the attachment to the mitochondrial inner membrane seen only rarely. Unlike other species, *F. neradi* contains numerous short cristae that are arranged transversely rather than longitudinally (Fig. 7O). Another prominent feature of the organelle is numerous patches of electron-dense DNA distributed throughout the mitochondrial matrix (Fig. 7K-O). Longitudinally and cross-sectioned cells show large mitochondrial profiles extending to the areas of the flagellar pocket and feeding apparatus (Figs 8B, D, 9F-I), although they do not reach the zone of flagellar attachment (Fig. 8A-E).

Analysis of longitudinally sectioned cells showed that the flagellar pocket is deep and morphologically similar in all analyzed species (Fig. 8A-E). Flagella arise from parallel basal bodies located in the proximal region of the flagellar pocket. Basal bodies are supported by the asymmetrically distributed ventral (Fig. 8B, E), intermediate (Fig. 8C), and dorsal (not shown) microtubular roots. Flagella of *L. lanifica*, *F. neradi*, *S. specki* invariably have

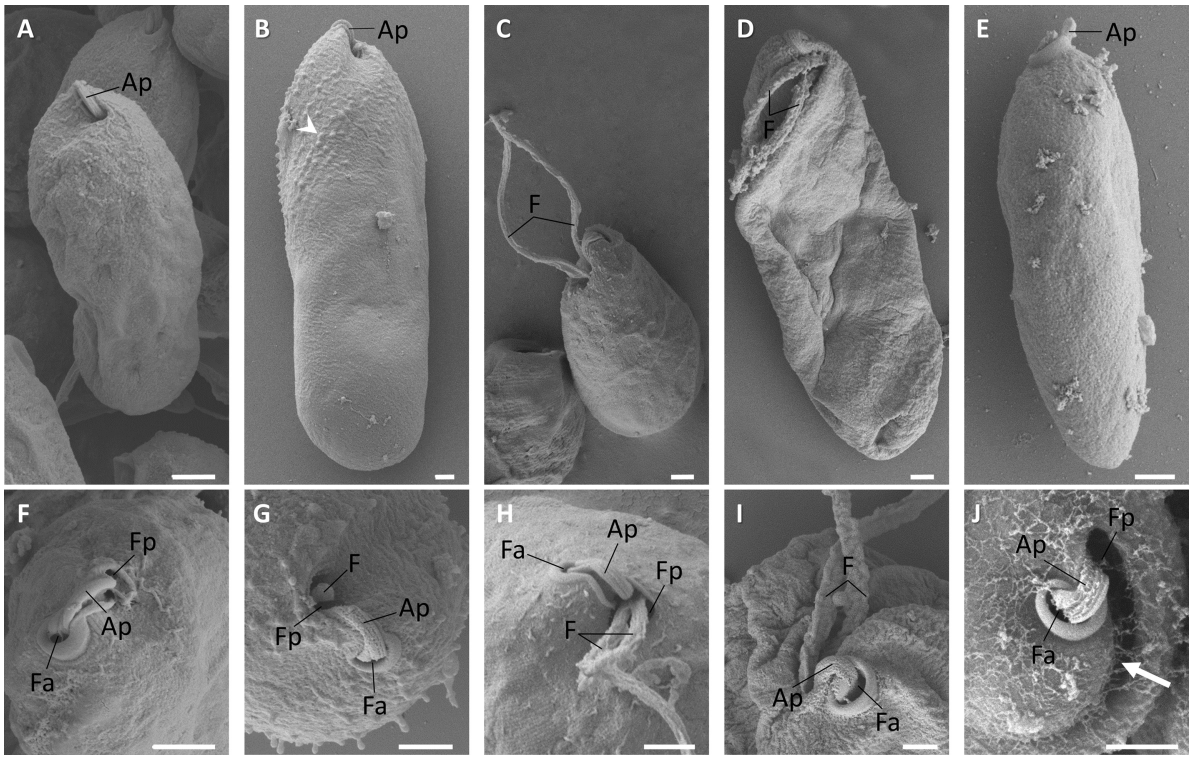

Figure 5. Scanning electron micrographs of *R. humris* (**A**, **F**), *R. serpens* (**B**, **G**), *L. lanifica* (**C**, **H**), *S. specki* (**D**, **I**), and *F. neradi* (**E**, **J**). **(A-E)** General appearance with apical papillum (Ap) and flagellum (F). Note a smooth cellular surface and pimples in the anterior part of *R. serpens* (arrowhead). **(F-J)** Detailed views of the anterior part showing subapical emergence of flagella from the pocket (Fp), and adjacent feeding apparatus (Fa) decorated with an apical papillum. Note a curved groove extended from the flagellar pocket in *F. neradi* (arrow). Scale bar = 1 μm.

conventional 9 + 2 axonemal arrangement of microtubules, and contain a prominent paraflagellar rod, which has a lattice-like structure (Fig. 8C-E, H-J). The paraflagellar rod joins the axoneme immediately after the distal transitional plate within the flagellar pocket, and runs along its length almost to the tip of the flagellum (Fig. 8A-E). The same structural organization is also preserved in fully developed flagella of starved *R. humris* and *R. serpens* (Fig. 8L, M), whereas, one or both flagella of trophic *Rhynchopus* cells are often rudimentary, with the paraflagellar rod and some axonemal tubules missing (Fig. 8F, G, K). Outer surfaces of the feeding apparatus, flagellar pocket and flagella are normally covered with a prominent glycocalyx (Fig. 8). In *R. humris*, they also coated with dense hairs (Fig. 8F, K, L), a feature that is in a less prominent form occasionally found also in the apex of *S. specki* and *L. lanifica* (data not shown).

Part of the flagellar pocket close to the basal bodies is marked with a complex of reinforcing microtubules (MTR) surrounded by a zone of exclusion along its entire length (Fig. 8A-E). The MTR extends into the pharyngeal complex of the feeding apparatus, which is located adjacent to the flagellar pocket, and supports both the flagellar pocket and pharyngeal complex along their length (data not shown). The pharyngeal complex opens with a cytostome and extends as a cytopharynx down into the cell reaching up to half of its length (Fig. 9F-J). Figure 6F shows a deep pharyngeal lumen at the level of the nucleus. In longitudinal view, pharynx appears as a horn-like structure (Fig. 9F-J). In all studied species, the feeding apparatus consists of fibrils arranged in a series of vanes (ribs) with supporting elements (rods) composed of fibrils and densely packed microtubules, and a row of longitudinally and transversely oriented microtubules on the opposite side (Fig. 9A-E). In its vicinity, the cytoplasm is surrounded by ER (Fig. 9A-E) and contains numerous vesicles that eventually seem to spread uniformly throughout the cell (Fig. 9F-J). Their content varies in terms of electron density and granulation and they tend to increase in size during spreading away from the feeding apparatus.

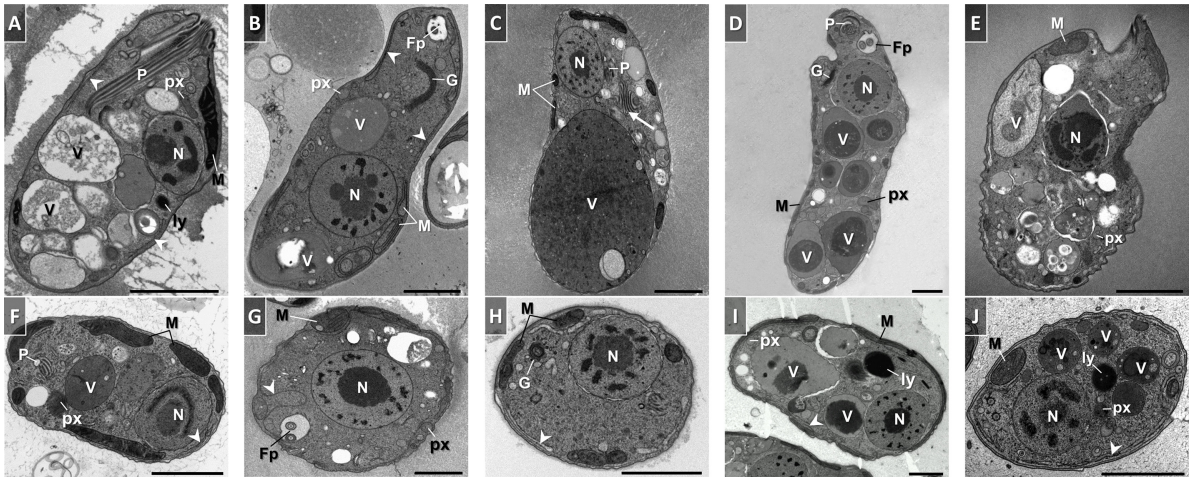

Figure 6. Transmission electron micrographs of *R. humris* (**A**, **F**), *R. serpens* (**B**, **G**), *L. lanifica* (**C**, **H**), *S. specki* (**D**, **I**), and *F. neradi* (**E**, **J**). (**A-E**) Longitudinal sections through the cell. (**F-J**) Transverse sections through the nucleus. (**B**) Nucleus (N) located in posterior part of the cell. (**A, C-E, G**) Nucleus in anterior region next to the bottom of the flagellar pocket (Fp), at the end of the pharyngeal lumen (P). Note large convoluted tubular vessels (*arrow*) near the ceasing pharyngeal lumen (P) and one large amorphous digestion vacuole (V) (**C**), numerous smaller digestion vacuoles of different contents (**A**, **B**, **D**, **E**), and little diverse vacuolar inclusions in the cytoplasm of all cells: peroxisomes (*px*), lysosomes (*ly*). Mitochondrial network (M) is located at the periphery; Golgi apparatus (G); ribosomes are electron-dense dots within the cytoplasm; *arrowheads* point to endoplasmic reticulum. Scale bar = 2 μm.

A single very large digestive vacuole is invariably present in the non-starved *L. lanifica* cells (Fig. 6C), while all other species possess numerous smaller vacuoles of different content (Fig. 6A-B, D-E). A conspicuous Golgi apparatus, with a variable number of both linear and circularized foci, is usually found in the perinuclear region (Fig. 10F-J). The cytoplasm is rich in free ribosomes, lysosomes, peroxisomes, small refractive granules, likely of reserve nature, and sparse endoplasmic reticula that are scattered among the food vacuoles (Figs 6, 7, 9, 10).

The nucleus is invariably large, spherical or oval, confined by a prominent nuclear membrane with readily visible pores (Fig. 10A-E). A persistent densely granular nucleolus is located either centrally or eccentrically within the nucleus, and may occupy as much as its third. The heterochromatin is highly condensed and distributed at the periphery of the homogeneous nucleoplasm (Fig. 10A-E). The nucleus commonly appears next to the bottom of the flagellar pocket, except for *R. serpens*, where it can be located both in the anterior and posterior region of the cell (Fig. 6).

A prominent feature of *L. lanifica* is the presence of large convoluted tubular vessels which lie near the proximal end of the feeding apparatus (Figs 6C, 9H). They look like a single, mostly O-shaped organelle, which somewhat resembles Golgi cisternae, but is larger and less electron-dense. Occasionally, numerous small membrane-bound droplets are seen within the vessels (data not shown). A direct connection between the pharynx and this organelle was not observed.

Discussion

Ribosomal RNA-based phylogenies confirm the existence of two main diplonemid clades, (provisionally) named Diplonemea and Eupelagonemea (Okamoto et al., submitted; this work). Not surprisingly, recent interest was directed to the hyperdiverse eupelagonemid diplonemids, as these may constitute one of the key players of the oceanic ecosystem (David and Archibald 2016; Flegontova et al. 2016; Gawryluk et al. 2016; Lukeš et al. 2015). Despite their enormous diversity, they are, at least on the level of 18S rRNA, quite uniform, which suggest a recent rapid speciation (Flegontova et al. 2016). However, exhaustive sampling of 18S rRNA sequences among Diplonemidae presented here shows that both *Hemistasia* and especially classic diplonemids contain previously unknown phylogenetic structuring and diversity. Classic diplonemids were traditionally composed of just two genera: *Rhynchopus* and *Diplonema* (Adl et al. 2012). Our 18S rRNA phylogeny supported by extensive sam-

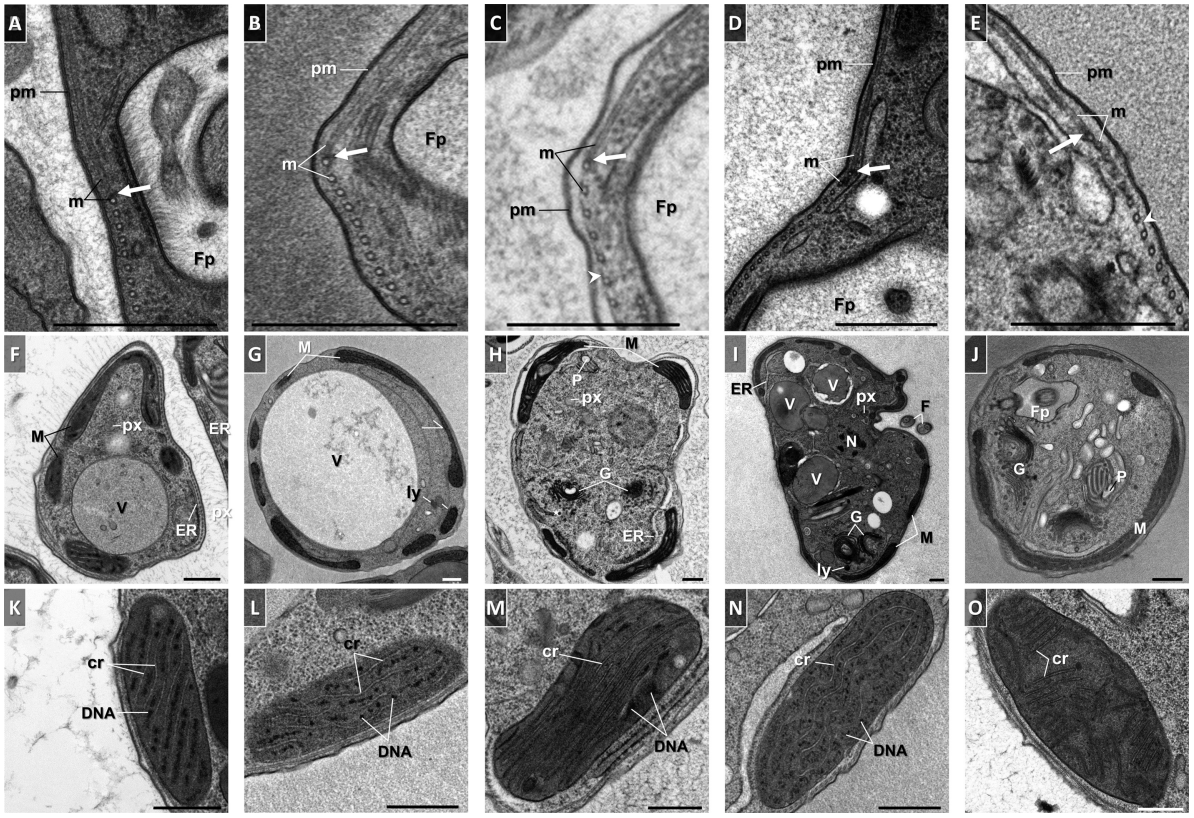

Figure 7. Transmission electron micrographs showing the surface ultrastructure and mitochondrial arrangement of *R. humris* (**A**, **F**, **K**), *R. serpens* (**B**, **G**, **L**), *L. lanifica* (**C**, **H**, **M**), *S. specki* (**D**, **I**, **N**), and *F. neradi* (**E**, **J**, **O**). (**A-E**) Cross section demonstrating plasma membrane (pm) and single row of microtubular corset (m) underneath it. Arrows point to the junction of microtubules in the region of the flagellar pocket (Fp). (**F-J**) Transverse section showing peripheral location of the mitochondrion (M). (**K-O**) Mitochondria displaying characteristic morphology: large lamellar cristae (cr) and abundant dense patches of DNA; nucleus (N); digestion vacuole (V); pharynx (P); Golgi apparatus (G); endoplasmic reticulum at ER; peroxisomes at *px*; lysosomes at *ly*. Ribosomes are electron-dense dots within the cytoplasm. *Arrowheads* point to fine lateral bridge. Scale bar = 0.5 μm.

pling of 'environmental' sequences, as well as newly described species, reveals the existence of at least five well-supported lineages. While *S. specki* and *F. neradi* fell into rare and species-poor clades, the third novel clade, represented here by the newly described *L. lanifica*, is the most diverse of the classic diplonemids and hence deserves further attention. Although most of the major diplonemid clades are robustly monophyletic, one should keep in mind that the 18S rRNA gene lacks the phylogenetic resolution to uncover their interrelationships and allow better understanding of the evolution of these remarkable protists. This situation shall eventually be improved by more extensive phylogenomic analyses employing the existence of several novel diplonemid species in culture and/or the power of single-cell transcriptomics.

All diplonemid species described to date share a common set of morphological and ultrastructural traits. The cells are sac-like but variable in shape, surrounded by a naked plasma membrane, which is supported by a tightly packed corset of parallel interconnected microtubules that follows a spiral course from the apex toward the posterior end. Such arrangement of the microtubular corset likely allows for extreme plasticity in shape and movement, as was observed in diplonemids and many euglenids (Arroyo et al. 2012; Jeuck and Arndt 2013; Simpson 1997; Swale 1973; Vickerman 1977; this work). The ER cisternae underlying the microtubular corset are likely involved in this active movement (Arroyo et al. 2012). As in the two other euglenozoan groups (Euglenida and Kinetoplastea), diplonemids carry a single peripheral

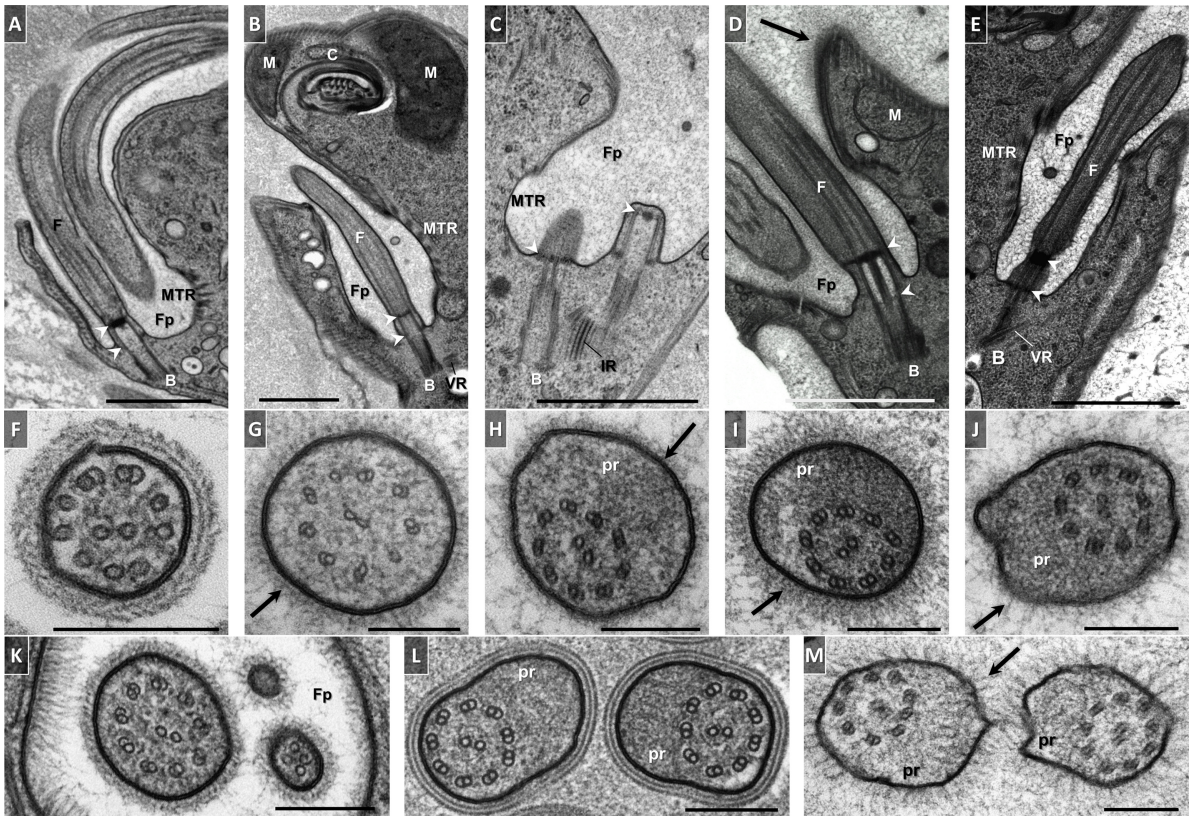

Figure 8. Ultrastructural architecture of the flagellar apparatus in *R. humris* (**A**, **F, K, L**), *R. serpens* (**B**, **G, M**), *L. lanifica* (**C**, **H**), *S. specki* (**D**, **I**), and *F. neradi* (**E**, **J**). (**A-E**) Longitudinal sections through flagella (F) and the area of flagellar attachment. In all strains, flagellar pocket (Fp) is deep and contains morphologically similar parallel basal bodies (B) located in the proximal region; ventral (VR) and intermediate (IR) roots. Flagellar pocket (Fp) is bordered by microtubular elements, reinforcing microtubules (MTR), which extend along and support the flagellar pocket and the pharyngeal wall (C). Note disrupted microtubular arrangement in the flagellar attachment zone and portions of large mitochondrion (M) in the areas of flagellar pocket (Fp) and feeding apparatus (C). *Arrowheads* indicate distal and proximal transitional plates. (**F-K**) Cross sections showing flagellar arrangement in trophic cells. Note characteristic 9 + 2 axonemal structure and lattice-like paraflagellar rod (pr) in *L. lanifica* (**H**), *F. neradi* (**I**), *S. specki* (**J**), and lack of B-tubules of the outer doublets and paraflagellar rod in *R. humris* (**F**) and *R. serpens* (**G**). (**K**) Likely, transitional stage of *R. humris*, where one of the flagella is fully developed yet missing paraflagellar rod and another appears as a rudiment. (**L-M**) Cross sections showing presence of conventional 9 + 2 arrangement plus paraflagellar rod in flagella of starved *R. humris* (**L**) and *R. serpens* (M). Note flagellar hairs in *R. humris* (**F, K, L**). *Arrows* point to glycocalyx. Scale bars = 1 μm (**A-E**) and 0.2 μm (**F-M**).

highly reticulated mitochondrion containing a large amount of mitochondrial DNA (Elbrächter et al. 1996; Faktorová et al. 2016; Marande et al. 2005; Maslov et al. 1999; Roy et al. 2007). However, as shown here, it is invariably arranged in numerous agglomerates lacking the kinetoplast-like structure characteristic for related trypanosomatids (Jensen and Englund 2012). Similarly dispersed distribution of the mitochondrial DNA was also described in euglenids and some bodonids (Hayashi and Ueda 1989; Lukeš et al. 2002).

Although we are the first to report a successful staining of the diplonemid mitochondria, allowing the observation of its complex structure, earlier 3D reconstruction and staining of the mitochondrial DNA provided evidence that this organelle is reticulated in other *Diplonema* and *Rhynchopus* species as well (Marande et al. 2005; Roy et al. 2007). In all ultrastructurally examined diplonemids, the single branched mitochondrion contains a few long lamellar cristae arranged in parallel (Elbrächter et al. 1996; Maslov et al. 1999; Porter 1973; Roy et al. 2007; Schnepf 1994; Vickerman 1977). The only known exception is *F. neradi* (this work), which not only contains a much higher number of cristae than other diplonemids, but also has them arranged

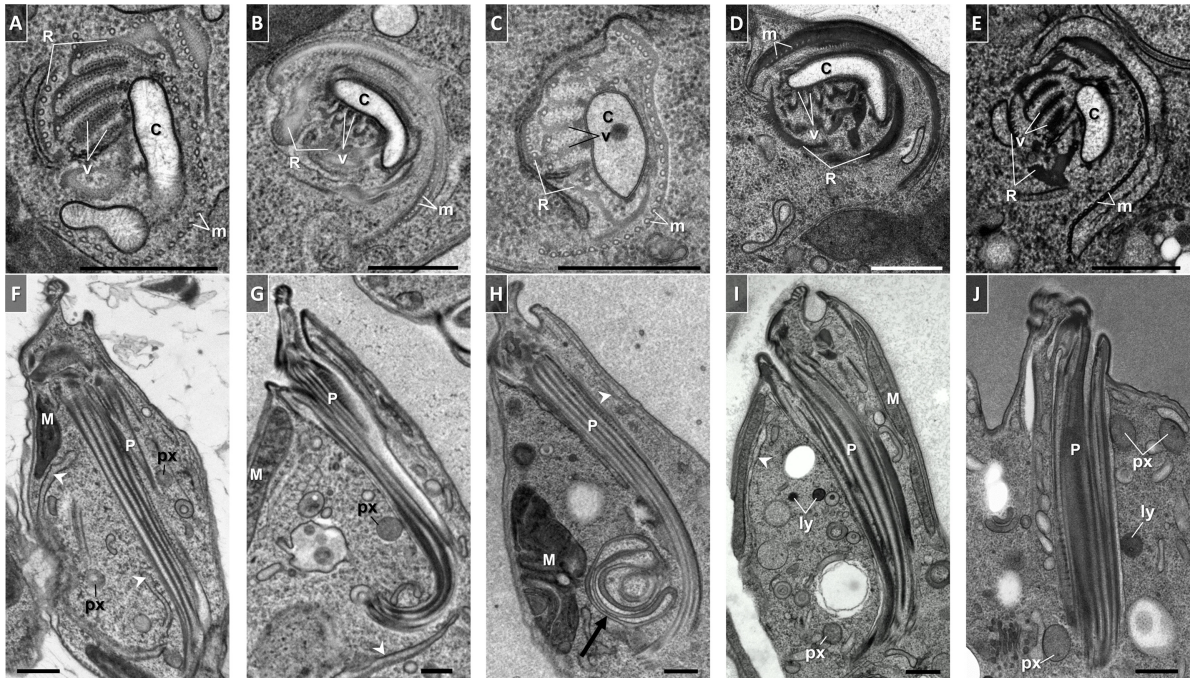

Figure 9. Ultrastructural architecture of the feeding apparatus in *R. humris* (**A**, **F**), *R. serpens* (**B**, **G**), *L. lanifica* (**C**, **H**), *S. specki* (**D**, **I**), and *F. neradi* (**E**, **J**). (**A-E**) Cross section showing the very top (**B, D**) and the intermediate part (**A, C, E**) of cytostome (C), which is the opening into the pharynx. Pharynx consists of a series of fibrils, the vanes (v), arranged in the form of a partial rosette, and supported by rods (R) and a row of microtubules (m). (**F-J**) Longitudinal section through the pharynx, which has a horn-like structure. The ribs forming the rosettes appear as a series of longitudinally-oriented dense lines. Note large convoluted tubular vessels (*arrow*) at the proximal end of pharynx (P) in **H**. *Arrowheads* indicate endoplasmic reticulum. The microbodies, numerous membrane-bounded vesicles, in early stages of formation surrounding the pharynx in the cytoplasm: peroxisomes at *px*; lysosomes at *ly*. Note portions of reticulated mitochondrion (M) surrounding the feeding apparatus and the density of ribosomes in the cytoplasm. Scale bar = 0.5 μm.

transversely rather than longitudinally. Other conspicuous cellular features of diplonemids are a prominent Golgi apparatus, which is much larger than in the sister kinetoplastids (Han et al. 2013) but similar to euglenids (Leedale 1982; Becker and Melkonian 1996), and the exceptionally large nucleoli within the vesicular nuclei.

The architecture of the cell apex equipped with characteristic flagellar and feeding apparatuses is nearly identical in all studied diplonemids. The flagellar complex has a basic configuration of two nearly parallel basal bodies and asymmetrically distributed microtubular roots (Elbrächter et al. 1996; Montegut-Felkner and Triemer 1994, 1996; Schnepf 1994). Such arrangement was also observed in bodonids (Brugerolle et al. 1979; Brugerolle 1985) and euglenids (Kivic and Walne 1984). In all diplonemids, the characteristic feeding apparatus is arranged parallel to the longitudinal cell axis and consists of fibrillar ribs arranged in the form of a partial rosette, supported by rod bundles and accompanying microtubules, which extend through the length of the pharynx (Montegut-Felkner and Triemer 1996; Porter 1973; Schuster et al. 1968). Another common feature is a conspicuous collar-like cytostome with an apical papillum, contiguous with the flagellar pocket (Larsen and Patterson 1990; Montegut-Felkner and Triemer 1996). The available SEM and TEM images clearly document two separate openings for the feeding apparatus and flagellar pocket in all diplonemids (Elbrächter et al. 1996; Montegut-Felkner and Triemer 1994, 1996; Porter 1973; Schuster et al. 1968; Triemer and Farmer 1991; this work), including *R. euleeides*, in which these were incorrectly interpreted as merged into a single opening (Roy et al. 2007). A feature distinguishing *R. humris* from the other diplonemids described herein is the presence of dense hair coat on both flagella and inside the cytostome and flagellar pocket. Flagellar hairs, although of varying fine structure, have been described in the diplone-

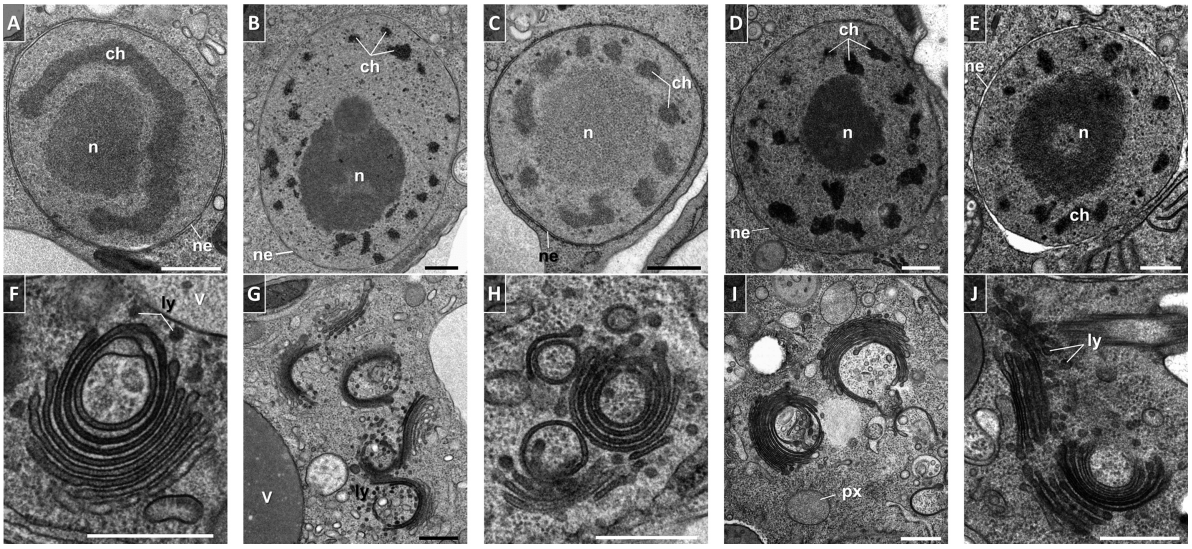

Figure 10. Transmission electron micrographs of nucleus and Golgi apparatus in *R. humris* (**A**, **F**), *R. serpens* (**B**, **G**), *L. lanifica* (**C**, **H**), *S. specki* (**D**, **I**), and *F. neradi* (**E**, **J**). **(A-E)** Section through large nuclei of vesicular pattern, with nuclear envelope (ne). Prominent centrally or eccentrically located nucleolus is surrounded by dense aggregations of chromatin (ch). (**F-J**) Cross sections of Golgi apparatus, which appears in either linear and/or circularized profiles, and is usually located adjacent to the nucleus/vacuoles (V). Peroxisomes at *px*; lysosomes at *ly*. Scale bar = 0.5 μm.

mid *H. phaeocysticola* (Elbrächter et al. 1996), and the kinetoplastids of the genera *Bodo* (Eyden 1977), *Cryptobia* (Vickerman 1977), *Rhynchobodo* (Brugerolle 1985) and *Phyllomitus* (Mylnikov 1986).

Members of the genus *Rhynchopus* studied so far produce two distinct stages during their life cycle: (i) big non-flagellated trophic cells with prominent cytoplasmic granulation and/or digestive vacuoles, which move by gliding, and (ii) smaller, fully motile stages equipped with two long flagella, which usually lack digestive vacuoles and cytoplasmic inclusions. Both stages were observed in *R. euleeides* (Roy et al. 2007), *R. serpens* and *R. humris* (this work), *Rhynchopus* sp. ATCC 50230 (Simpson 1997) and in several other *Rhynchopus* species (von der Heyden et al. 2004), whereas for *R. coscinodiscivorus* (Schnepf 1994) and an *Isonema*-like (a junior synonym of *Diplonema*; Triemer and Ott, 1990) flagellate (Kent et al. 1987), only a trophic stage has been described. This can be explained by the fact that no observations were made under starvation conditions, which are known to trigger the emergence of the swimming stages (von der Heyden et al. 2004; this study). Since all other known diplonemid species have two permanently protruding flagella (Elbrächter et al. 1996; Larsen and Patterson 1990; Porter 1973; Schuster et al. 1968; Triemer and Ott 1990; this work), we suggest that the existence of non-flagellated trophic stages is a discriminatory morphological feature for the genus *Rhynchopus*.

Flagellar stubs in trophic *Rhynchopus* cells often lack ordered axonemes with 9 + 2 microtubular arrangement (Schnepf 1994; Simpson 1997; this work). However, long flagella in their respective swimming stages develop regular axonemes accompanied by paraflagellar rods, which likely helps hydrodynamic propulsion (Hughes et al. 2012). This was shown for *Rhynchopus* sp. ATCC 50230 (Simpson 1997), *R humris* and *R. serpens* (this work), while ultrastructural data are missing for swimming stages of *R. euleeides* (Roy et al. 2007), *R. coscinodiscivorus* (Schnepf 1994) and the *Isonema*-like flagellate (Kent et al. 1987). Paraflagellar rods are absent in trophic stages of *D. nigricans* (Schuster et al. 1968), *D. papillatum* (Porter 1973), and *D. ambulator* (Montegut-Felkner and Triemer 1994) in agreement with the apomorphy suggested for diplonemids by Adl et al. (2012). Here, we show that the flagella in trophic *F. neradi*, *S. specki* and *L. lanifica* cells are paraflagellar rod-bearing. While the latter diplonemid is capable of fast swimming under starvation conditions, the functions of flagella in *F. neradi* and *S. specki* should be further investigated, since these are used neither for substrate attachment nor for cell propulsion. However, we might have failed to find conditions

under which cells with long swimming flagella are produced.

Diplonemids studied herein can be distinguished by their characteristic morphology under nutrient-rich conditions. However, in every species the size, shape, length of flagella and cytoplasmic granulation are subject to high variability when nutrients are limited. Hence, species determination in natural samples or under different conditions may be difficult or even impossible. Distantly related species may exhibit similar morphology as in case of *L. lanifica* and the 4sb cell belonging to the Eupelagonemidae clade (Gawryluk et al. 2016; Okamoto et al., submitted; this work). The same is true for the swimming stages of different *Rhynchopus* species (Roy et al. 2007; this work). At the same time, the subcellular organization is strikingly similar among the representatives of different diplonemid genera as described in this work and elsewhere (Roy et al. 2007; Schnepf 1994; Triemer and Ott 1990) and hence, cannot aid species identification. Consequently, the determination and systematics of diplonemids, at least at the species level, will rather have to rely on the sequence data.

Due to little interspecies difference among *Rhynchopus* and their great morphological variability depending on nutrient availability, we argue that identification of species should not be based solely on morphological traits, and that observations under both nutrient-rich and starvation conditions are needed. The freshwater lifestyle of *R. amitus* suggests that this species is different from *R. humris* and *R. serpens*. The size and shape of *R. coscinodiscivorus* (pear-shaped; 20-25 $\times$ 10-12 μm) are similar to those of *R. serpens* (elongated, pear-shaped; 21.3-28.7 $\times$ 7.2-9 μm) but the 18S rRNA sequence is unavailable for the former species, precluding their more detailed comparison, whereas parasitizing or predation on diatoms is not known for *R. serpens*. Nevertheless, based on the cell morphology, we conclude that *L. lanifica*, *F. neradi* and *S. specki* are different species from previously described non-sequenced diplonemids. All three species are noticeably smaller, even under nutrient-rich conditions, than *D. metabolicum* (30-48 μm long) and *D. nigricans* (40-50 μm long), and never produce conical cells with broad anterior and tapered posterior ends (Schuster et al., 1968; Larsen and Patterson 1990). The length of their flagella when in the trophic phase readily distinguishes them from all described *Rhynchopus* species.

All diplonemids described in this study were isolated as free-swimming cells from water samples. However, a *Rhynchopus* isolate with 99% of 18S rRNA sequence identity to *R. humris* (Fig. 1), was reported to cause massive infections of the *Nephrops norvegicus* lobster (von der Heyden et al. 2004). Since our culture was established from a free-swimming motile cell, we propose that it may represent a dispersive and/or invasive stage, while the trophic stage develops under nutrient-rich conditions, such as are inside the host. It seems that parasitism, at least transient, as well as predation, are common life strategies for members of the genus *Rhynchopus*. Indeed, several species were found to parasitize crabs, lobsters and clams (Bodammer and Sawyer 1981; Kent et al. 1987; von der Heyden et al. 2004), while *R. coscinodiscivorus* predates/parasitizes on diatoms by invading the frustule (Schnepf 1994). So far, the literature refers to diplonemids mostly as to parasites or epibionts of plants and invertebrates or as predators of algae rather than bacterivores or detritus feeders (Vickerman 2000). Specifically, *D. ambulator* is involved in *Cryptocoryne* plant disease (Triemer and Ott 1990), *D. papillatum* is associated with drifting eelgrass (Porter 1973), *D. metabolicum* feeds on leaves of the *Halophila* seagrass (Larsen and Patterson 1990), and *H. phaeocysticola* feeds on diatoms, dinoflagellates and copepods (Elbrächter et al. 1996). Alternatively, *D. ambulator* and *R. euleeides* may also graze bacteria and ingest detritus particles (Larsen and Patterson 1990; Roy et al. 2007). However, new extensive sequence data from the pelagic samples (Flegontova et al. 2016; Gawryluk et al. 2016) point to the free-living heterotrophic life style of most species.

Taxonomic Summary

Phylum Euglenozoa Cavalier-Smith 1981, emend. Simpson 1997

Class Diplonemea Cavalier-Smith 1993, emend. Simpson 1997

Genus ***Rhynchopus*** Skuja (1948)

Rhynchopus humris sp. n. Tashyreva, Prokopchuk, Horák and Lukeš (2018)

Description: trophic cells elongated, dorsoventrally flattened, narrowed at both ends; 12.5-16.4 μm (14.5 $\pm$ 1.2 μm; n = 25) long and 3.3-5.1 μm (4.2 $\pm$ 0.59 μm; n = 25) wide; prominent granulation throughout cytoplasm. Short flagellar stubs with disordered axonemes, lacking paraflagellar rods, concealed inside flagellar pocket. Highly metabolic, move by gliding on surfaces. Fast

swimming stage in starved cultures; dimensions 7.2 × 3.2 μm; dorsoventrally compressed; cytoplasmic inclusions absent. Flagella up to 2.5 times of body length, inserted subapically, both with regular axonemes and paraflagellar rods. Anterior flagellum loops around cell apex; posterior flagellum stretched. Nucleus in central part proximally to cell periphery; mitochondrial cristae arranged longitudinally; flagella pocket hairs. No cysts and extrusomes.

Etymology: The species name is a Czech word for lobster, which is the host of a species with 99% 18S rRNA sequence identity to YPF1608.

Type strain: YPF1608

Type material: hapantotype (OsO_4-fixed slide) and genomic DNA sample deposited at the protistological collection of the Institute of Parasitology, Biology Centre, Czech Academy of Sciences, České Budějovice, no. IPCAS Prot 37

Gene sequence: MF422204, 18S rRNA gene, partial sequence.

Type locality: sand filter of 'D-1′ tank in Enoshima Aquarium, Fujisawa, Kanagawa, Japan.

Rhynchopus serpens sp. n. Tashyreva, Prokopchuk, Horák and Lukeš (2018)

Description: trophic cell cells elongated, dorsoventrally flattened, tapered at the anterior, rounded and widened posteriorly; numerous cytoplasmic inclusions in posterior half; 21.3-28.7 μm (26.0 ± 1.7 μm; n = 25) long and 7.2-9 μm (8.0 ± 0.6 μm; n = 25) wide. Short flagellar stubs with disordered axonemes, lacking paraflagellar rods, concealed inside flagellar pocket. Highly metabolic, move by gliding on surfaces. Swimming stage in starved cultures small (13.5 × 3.7 μm), cytoplasmic granulation reduced or absent, dorsoventrally compressed; slow swimming with both flagella stretched along body or fast swimming cells with anterior flagellum forming loop and posterior flagellum stretched. Flagella up to 2.5 times of body length, inserted subapically, both with regular axonemes and paraflagellar rods. Nucleus position variable; mitochondrial cristae arranged longitudinally. No cysts and extrusomes.

Etymology: The species name describes the crawling movement of the cells.

Type strain: YPF1515

Type material: hapantotype (OsO_4-fixed slide) and genomic DNA sample deposited at the protistological collection of the Institute of Parasitology, Biology Centre, Czech Academy of Sciences, České Budějovice, no. IPCAS Prot 38

Gene sequence: MF422195, 18S rRNA gene, partial sequence.

Type locality: Kaiike-lagoon, Koshikijima Island, Satsuma-Sendai, Kagoshima, Japan (31°51′36″N, 129°52′29″E), surface water.

Phylum Euglenozoa Cavalier-Smith 1981, emend. Simpson 1997

Class Diplonemea Cavalier-Smith 1993, emend. Simpson 1997

Genus ***Lacrimia*** gen. n. Tashyreva, Prokopchuk, Horák and Lukeš (2018)

Marine diplonemids distinguished from similar genera by molecular phylogenetic analyses.

Type species: *Lacrimia lanifica*.

Lacrimia lanifica sp. n. Tashyreva, Prokopchuk, Horák and Lukeš (2018)

Description: cells in well growing cultures nearly isodiametric but often teardrop-shaped, large digestive vacuoles at posterior end, narrowed anterior end; 10.4-15.3 μm (13.1 ± 1.3 μm; n = 25) long and 7.3-10.5 μm (8.7 ± 0.74 μm; n = 25) wide. Two subapical subequal body-length flagella, with regularly arranged axonemes and paraflagellar rods. Cells homogeneously suspended, metabolic, maintaining constant rotation movements; gliding along surface by attaching with longer flagellum. Cells in aged and starved cultures elongated and small (7.5 × 3.6 μm), lacking food vacuoles. Occasional fast swimming cells move in straight line through spiral oscillating movement. Nucleus in anterior half; mitochondrial cristae arranged longitudinally. No cysts and extrusomes produced.

Etymology: The name (feminine) reflects the tear-drop shape (lacrima) and spinning movement (lanifica)

Type strain: YPF1601

Type material: hapantotype (OsO_4-fixed slide) and genomic DNA sample deposited at the protistological collection of the Institute of Parasitology, Biology Centre, Czech Academy of Sciences, České Budějovice, no. IPCAS Prot 39

Gene sequence: MF422199, 18S rRNA gene, partial sequence

Type locality: Tokyo Bay (35°19′10″N, 139°39′04″E), surface water.

Phylum Euglenozoa Cavalier-Smith 1981, emend.

Simpson 1997

Class Diplonemea Cavalier-Smith 1993, emend. Simpson 1997

Genus ***Sulcionema*** gen. n. Tashyreva, Prokopchuk, Horák and Lukeš (2018)

Marine diplonemids distinguished from similar genera by molecular phylogenetic analyses.

Type species: *Sulcionema specki*.

Sulcionema specki sp. n. Tashyreva, Prokopchuk, Horák and Lukeš (2018)

Description: cells in nutrient-rich medium noticeably flattened with tapered, slightly crooked anterior along with rounded posterior ends, conspicuous cytoplasmic granulation; 23.7-33.3 μm (27.6 ± 2.1 μm; n = 25) long and 5.8-9.6 μm (7.4 ± 0.9 μm; n = 25) wide. Two equal to subequal flagella third of body length, with paraflagellar rods and regular axonemes. Cells suspended in medium, highly metabolic, flagella support only erratic movement. Starved cells reduce size to 16.3 × 5 μm, morphologically variable, cytoplasmic granulation reduced or absent. Swimming stage, cysts and extrusomes not observed. Nucleus mostly in posterior half; mitochondrial cristae arranged longitudinally.

Etymology: The generic name (neuter) reflects in Latin the sausage-like shape of the cells, and the species name in German ("bacon") refers to lipid-like cell inclusions.

Type strain: YPF1618

Type material: hapantotype (OsO_4-fixed slide) and genomic DNA sample deposited at the protistological collection of the Institute of Parasitology, Biology Centre, Czech Academy of Sciences, České Budějovice, no. IPCAS Prot 40

Gene sequence: MF422201, 18S rRNA gene, partial sequence.

Type locality: Oura Beach, Shikinejima Island, Tokyo, Japan (34°19′48″N, 139°12′29″E), surface water.

Phylum Euglenozoa Cavalier-Smith 1981, emend. Simpson 1997

Class Diplonemea Cavalier-Smith 1993, emend. Simpson 1997

Genus ***Flectonema*** gen. n. Tashyreva, Prokopchuk, Horák and Lukeš (2018)

Marine diplonemids distinguished from similar genera by molecular phylogenetic analyses. Type species: *Flectonema neradi.*

Flectonema neradi gen. n., sp. n. Tashyreva, Prokopchuk, Horák and Lukeš (2018)

Description: cells in nutrient-rich medium dorsoventrally flattened, constricted at both ends, thin and crooked, with granulation in the posterior region; 15.9-20.9 μm (18.3 ± 1.45 μm; n = 25) long and 3.5-5.8 μm (4.0 ± 0.6 μm; n = 25) wide; slowly glide on surfaces, display pronounced metaboly, attach to surfaces with one flagellum and rotate. Two equal subapical flagella fifth of body length, both with regular axonemes and paraflagellar rods. No fast swimming stages or cysts in old batch cultures and starvation medium. Starved cells short and rounded, some with constricted posterior ends, 6.3 × 3.1 μm, lack cytoplasmic inclusions. Nucleus position variable; mitochondrial cristae arranged transversely; opening of flagellar pocket extended into curved groove. Extrusomes not observed.

Etymology: The name (neuter) is derived from the bent shape (flecto-), the species name is after Thomas Nerad, the isolator of the strain.

Type strain: ATCC50224

Type material: hapantotype (OsO_4-fixed slide) and genomic DNA sample deposited at the protistological collection of the Institute of Parasitology, Biology Centre, Czech Academy of Sciences, České Budějovice, no. IPCAS Prot 41.

Gene sequence: AF119812, 18S rRNA gene, partial sequence.

Type locality: Gaithersburg, Maryland, USA.

Methods

Isolation and cultivation: Samples from aquaria, lagoon and sandy beach seawater were collected around Japan. The details on the collected samples are summarized in the Supplementary Material Table SA2. The samples were inoculated into seawater-based Hemi medium (designed in this study), containing 3.6% sea salts (Sigma-Aldrich), enriched with 1% (v/v) heat-inactivated horse serum (Sigma-Aldrich) and 0.025 g/l LB broth powder (Amresco). The medium was supplemented with 10 μl/ml antibiotics cocktail (P4083, Sigma-Aldrich) and sterilized by filtering through a 0.22 μm filter. The samples were then incubated at 20 °C. Possible diplonemid cells were isolated under the inverted microscope CKX31 (Olympus) using glass microcapillaries. In total, 18 strains from isolated single cells were established. A culture of *Diplonema* sp. 2 (ATCC 50224) was obtained from ATCC. All cultures were grown axenically at 15 or 20 °C in antibiotic-free Hemi medium. Additionally, for some experiments, the cultures were starved by incubation in a medium diluted 1:10 with seawater for up to 10 days.

DNA isolation, PCR amplification and sequencing: Total genomic DNA was isolated from cultures with DNeasy Blood & Tissue Kit (Qiagen) following the protocol A as described by the manufacturer. The nearly full-size 18S rRNA gene was amplified with universal eukaryotic primers SA (5′-AACCTGGTTGATCCTGCCAGT-3′) and SB (5′-TGATCCTCCTGCAGGTCCACCT-3′), the amplicons were purified and sequenced.

Phylogenetic analyses: 18S rRNA sequences of novel diplonemid species described here were added to the exhaustive dataset of euglenozoan 18S rRNA extracted from public databases using the EukRef approach (eukref.org). The dataset was aligned together with newly sequenced cultures using the genafpair algorithm as implemented in Mafft v7. 305b (Katoh and Standley 2013). Ambiguous regions were removed by eye in Seaview 4 (Gouy et al. 2010). At this step, we created three datasets differing by outgroup composition. In dataset K, only kinetoplastids were used as an outgroup. This dataset composed of 133 taxa and 2000 nucleotide sites. In datasets E (149 taxa and 1835 sites) and H (152 taxa, 1835 sites) outgroups were expanded by the addition of euglenids and heteroloboseans and euglenids, respectively. The best fitting model of evolution for each dataset, as well as maximum likelihood phylogenies under these selected models, were estimated using IQ-Tree (Nguyen et al. 2015) with thorough non-parametric bootstrap analysis of 1,000 replicates as a measure of branching support. Robustness of observed topologies was also tested using Bayesian posterior probabilities as inferred by Phylobayes 4.1 (Lartillot et al. 2009) under the empirical mixture model C40 combined with exchange rates as defined by GTR matrix (C40 + GTR model). Two independent MCMC chains were ran until convergence was reached (i.e. maximum observed discrepancy was lower than 0.1 and effective sample size of observed statistics was at least 100). Alternative hypotheses on topologies of selected taxa (see Results) were tested using an approximately unbiased (AU) test in Consel (Shimodaira and Hasegawa 2001). For this, we first forced alternative topologies, re-optimized the ML tree and computed per-site log-likelihood scores in RAxML 8.28b (Stamatakis 2014).

Light microscopy: For imaging, live cells were trapped between a slide and coverslip with edges sealed either with nail polish or immobilized by suspending in 0.5 to 1% ultralow gelling agarose solution (Sigma). Microscopy slides for agarose-immobilized cells were prepared according to Reize and Melkonian (1989). Light microscopy observations were performed with either Olympus BX53 equipped with differential interference contrast (DIC) or Zeiss Primovert. Videos and images were taken with a DP72 microscope digital camera at 1600 × 1200-pixel resolution using CellSens software v. 1.11 (Olympus). The images were processed using GIMP v. 2.8.14, Irfan view v. 4.41 and Image J v. 1.51 software.

Fluorescence staining and microscopy: For DNA staining, cell pellets were fixed with seawater-based Parducz fixative consisting of 6:1 volumes of 2% OsO_4 and saturated $HgCl_2$ solutions (Párducz 1967) for 15 min, and washed thoroughly with distilled water. Cell suspensions were applied on glass slides, air-dried, and mounted in ProLong Gold antifade reagent with 4′,6-diamidino-2-phenylindole, or DAPI (Life Technologies). For mitochondrial staining, live cells in serum-free medium were treated for 30 min with (i) 100 or 200 nM MitoTracker Green FM, (ii) 100 or 500 nM MitoTracker Red CMXRos, (iii) 60 nM tetramethylrhodamine ethyl ester (TMRE), and (iv) 2, 6, 10 or 20 μM $DiOC_6(3)$ either with or without addition of 5% v/v dimethyl sulfoxide (DMSO) (all dyes Life Technologies, USA). Slides were prepared as described above and observed with an AxioPlan 2 fluorescence microscope (Zeiss). In addition, we attempted to visualize mitochondria with immunofluorescence assay targeting mitochondrial heat shock protein (HSP) 70 with antibodies generated against *Trypanosoma brucei* HSP70, as described in Zíková et al. (2009).

Electron microscopy: For scanning electron microscopy (SEM), pellets were fixed with the above-described Parducz fixative (pH 7.4) either alone or followed by instantaneous freezing in liquid nitrogen and freeze-drying at -60 °C under high vacuum for 12 hours following a procedure described elsewhere (Small and Marszalek 1969). Alternatively, fixed cells were adhered to poly-*L*-lysine coated glass coverslips and dehydrated in an increasing gradient of acetone (30% to 100%), in sets of 15 min, and critical point dried using CO_2. Dehydrated samples were then transferred onto SEM specimen stubs, coated with gold/palladium in Sputter Coater Polaron chamber, and examined using a JEOL JSM-7401-F microscope at an accelerating voltage of 4 kV. Conventional fixation procedure with 4% paraformaldehyde or 2.5% glutaraldehyde followed by the dehydration in ethanol series could not be used, as it resulted in near-complete disintegration of cells. For transmission electron microscopy (TEM), samples were prepared by high pressure freezing technique (HPF) as described previously (Yurchenko et al. 2014). Ultrathin sections were observed in a JEOL 1010 TEM microscope at accelerating voltage of 80 kV. Images were captured with an Olympus Mega View III camera.

Acknowledgements

This work was supported by the European Research CouncilCZ LL1601 (to JL), the Czech Grant Agency projects Nos. P506-12-P9 (to AH) and 14-23986S (to JL), Czech-BioImaging RI project (LM2015062 funded by MEYS CR) and grant from the Japanese Society for the Promotion of Science No. 26840133 (to AY). We thank Dr. S Tsuchida (JAMSTEC) and Messers M Kawato (JAMSTEC), H Kishi (Satsumasendai City Office), Y Suzuki, S Nemoto and M Sugimura (Enoshima Aquarium) for providing a part of the samples.

Appendix A.

Table A1A. Trophic cells in nutrient-rich medium.

Species	*R. humris*	*R. serpens*	*L. lanifica*	*S. specki*	*F. neradi*
Cell shape	elongated, terminally narrowed	elongated, acute anterior and round posterior ends	nearly round or teardrop-shaped	elongated, laterally flattened	elongated, posteriorly rounded, bent
Cell size, μm[a]	12.5-16.4 × 3.3-5.1	21.3-28.7 × 7.2-9	10.4-15.3 × 7.3-10.5	23.7-33.3 × 5.8-9.6	15.9-20.9 × 3.5-5.8
Flagella	stubs, buried in flagellar pocket	stubs, buried in flagellar pocket	subequal, as body length	subequal, a third of body length	equally long, a fifth of body length
Movement	gliding, metabolic	gliding, metabolic	rotation, gliding with flagellum, metabolic	erratic, metabolic	gliding, rotation, metabolic
Cytoplasmic inclusions	big vesicles	big posterior vesicles	big posterior vacuole	conspicuously big vesicles	posterior vesicles

[a]measured in extended state.

Table A1B. Cells after starvation treatment.

Species	*R. humris*	*R. serpens*	*L. lanifica*	*S. specki*	*F. neradi*
Cell shape	elongated, terminally narrowed	elongated with both ends rounded	oval	elongated with both ends rounded	elongated or rounded
Cell size, μm[a]	7.2 × 3.2	13.5 × 3.7	7.5 × 3.6	16.3 × 5	6.3 × 3.1
Flagella	unequally long, 2 times of body length	unequally long, 2 to 2.5 times of body length	unequally long, 1 to 2.5 times of body length	subequal, a third of body length	equally long, a fifth of body length
Movement	fast swimming, metabolic	fast swimming, metabolic	rotation, gliding, metabolic, swimming	erratic, metabolic	gliding, rotation, metabolic
Cytoplasmic inclusions	absent	absent	absent	small or absent	small or absent

[a]smallest measured cells.

Appendix B. Supplementary Data

Supplementary data associated with this article can be found, in the online version, at https://doi.org/10.1016/j.protis.2018.02.001.

References

Adl SM, Simpson AGB, Lane CE, Lukeš J, Bass D, Bowser SS, Brown MW, Burki F, Dunthorn M, Hampl V, Heiss A, Hoppenrath M, Lara E, Le Gall L, Lynn DH, McManus H, Mitchell EAD, Mozley-Stanridge SE, Parfrey LW, Pawlowski J, Rueckert S, Shadwick L, Shadwick L, Schoch CL, Smirnov A, Spiegel FW (2012) The revised classification of eukaryotes. J Eukaryot Microbiol **59**:429–493

Arroyo M, Heltai L, Millan D, DeSimone A (2012) Reverse engineering the euglenoid movement. Proc Natl Acad Sci USA **109**:17874–17879

Becker B, Melkonian M (1996) The secretory pathway of protists: spatial and functional organization and evolution. Microbiol Rev **60**:697–721

Bodammer JE, Sawyer TK (1981) Aufwuchs protozoa and bacteria on the gills of the rock crab, *Cancer irroratus* say: a survey by light and electron microscopy. J Protozool **28**:35–46

Brugerolle G (1985) Des trichocystes chez les bodonides, un caractè phylogénétique supplementaire entre Kinetoplastida et Euglenida. Protistologica **21**:339–348

Brugerolle G, Lom J, Nohýnkova E, Joyon L (1979) Comparaison et évolution des structures cellulaires chez plusieurs espèces de Bodonidés et Cryptobiidés appartenent aux genres *Bodo*, *Cryptobia* et *Trypanoplasma* (Kinetoplastida, Mastigophora). Protistologica **15**:197–221

Busse I, Preisfeld A (2002) Phylogenetic position of *Rhynchopus* sp. and *Diplonema ambulator* as indicated by analyses of euglenozoan small subunit ribosomal DNA. Gene **284**:83–91

David V, Archibald JM (2016) Evolution: plumbing the depths of diplonemid diversity. Curr Biol **26**:R1290–R1292

de Vargas C, Audic S, Henry N, Decelle J, Mahé F, Logares R, Lara E, Berney C, Le Bescot N, Probert I, Carmichael M, Poulain J, Romac S, Colin S, Aury J-M, Bittner L, Chaffron S, Dunthorn M, Engelen S, Flegontova O, Guidi L, Horák A, Jaillon O, Lima-Mendez G, Lukeš J, Malviya S, Morard R, Mulot M, Scalco E, Siano R, Vincent F, Zingone A, Dimier C, Picheral M, Searson S, Kandels-Lewis S, Tara Oceans Coordinators, Acinas SG, Bork P, Bowler C, Gorsky G, Grimsley N, Hingamp P, Iudicone D, Not F, Ogata H, Pesant S, Raes J, Sieracki ME, Speich S, Stemmann L, Sunagawa S, Weissenbach J, Wincker P, Karsenti E (2015) Ocean plankton. Eukaryotic plankton diversity in the sunlit ocean. Science **348**:1261605

Elbrächter M, Schnepf E, Balzer I (1996) *Hemistasia phaeocysticola* (Scherffel) comb. nov., redescription of a free-living, marine, phagotrophic kinetoplastid flagellate. Arch Protistenkd **147**:125–136

Eloe EA, Shulse CN, Fadrosh DW, Williamson SJ, Allen EE, Bartlett DH (2011) Compositional differences in particle-associated and free-living microbial assemblages from an extreme deep-ocean environment. Environ Microbiol Rep **3**:449–458

Eyden BP (1977) Morphology and ultrastructure of *Bodo designis* Skuja 1948. Protistologica **13**:169–179

Faktorová D, Dobáková E, Peña-Diaz P, Lukeš J (2016) From simple to supercomplex: mitochondrial genomes of euglenozoan protists. F1000Research **5**:392

Flegontova O, Flegontov P, Malviya S, Audic S, Wincker P, de Vargas C, Bowler C, Lukeš J, Horák A (2016) Extreme diversity of diplonemid eukaryotes in the ocean. Curr Biol **26**:3060–3065

Gawryluk RMR, Del Campo J, Okamoto N, Strassert JFH, Lukeš J, Richards TA, Worden AZ, Santoro AE, Keeling PJ (2016) Morphological identification and single-cell genomics of marine diplonemids. Curr Biol **26**:3053–3059

Gouy M, Guindon S, Gascuel O (2010) SeaView Version 4: a multiplatform graphical user interface for sequence alignment and phylogenetic tree building. Mol Biol Evol **27**:221–224

Griessmann K (1913) Über marine Flagellaten. Arch Protistenkd **32**:1–78

Han HM, Bouchet-Marquis C, Huebinger J, Grabenbauer M (2013) Golgi apparatus analyzed by cryo-electron microscopy. Histochem Cell Biol **140**:369–381

Hayashi Y, Ueda K (1989) The shape of mitochondria and the number of mitochondrial nucleoids during the cell cycle of *Euglena gracilis*. J Cell Sci **93**:565–570

Hughes LC, Ralston KS, Hill KL, Zhou ZH (2012) Three-dimensional structure of the trypanosome flagellum suggests that the paraflagellar rod functions as a biomechanical spring. PLoS ONE **7**:e25700, http://dx.doi.org/10.1371/journal.pone.0025700

Jensen RE, Englund PT (2012) Network news: the replication of kinetoplast DNA. Annu Rev Microbiol **66**:473–491

Jeuck A, Arndt H (2013) A short guide to common heterotrophic flagellates of freshwater habitats based on the morphology of living organisms. Protist **164**:842–860

Katoh K, Standley DM (2013) MAFFT Multiple Sequence Alignment Software version 7: improvements in performance and usability. Mol Biol Evol **30**:772–780

Kent ML, Elston RA, Nerad TA, Sawyer TK (1987) An *Isonema*-like flagellate (Protozoa: Mastigophora) infection in larval geoduck clams, *Panope abrupta*. J Invertebr Pathol **50**:221–229

Kiethega GN, Yan Y, Turcotte M, Burger G (2013) RNA-level unscrambling of fragmented genes in *Diplonema* mitochondria. RNA Biol **10**:301–313

Kivic PA, Walne PL (1984) An evaluation of a possible phylogenetic relationship between the Euglenophyta and Kinetoplastida. Orig Life **13**:269–288

Lara E, Moreira D, Vereshchaka A, López-García P (2009) Pan-oceanic distribution of new highly diverse clades of deep-sea diplonemids. Environ Microbiol **11**:47–55

Larsen J, Patterson DJ (1990) Some flagellates (Protista) from tropical marine sediments. J Nat Hist **24**:801–937

Lartillot N, Lepage T, Blanquart S (2009) PhyloBayes 3: a Bayesian software package for phylogenetic reconstruction and molecular dating. Bioinformatics **25**:2286–2288

Leedale GF (1982) Ultrastructure. In Buetow D (ed) The Biology of *Euglena*. Academic Press, New York, pp 1–27

López-García P, Vereshchaka A, Moreira D (2007) Eukaryotic diversity associated with carbonates and fluid seawater interface in Lost City hydrothermal field. Environ Microbiol **9**:546–554

Lukeš J, Flegontova O, Horák A (2015) Diplonemids. Curr Biol **25**:R702–R704

Lukeš J, Guilbride DL, Votýpka J, Zíková A, Benne R, Englund PT (2002) Kinetoplast DNA network: evolution of an improbable structure. Eukaryot Cell **1**:495–502

Marande W, Burger G (2007) Mitochondrial DNA as a genomic jigsaw puzzle. Science **318**:415

Marande W, Lukeš J, Burger G (2005) Unique mitochondrial genome structure in diplonemids, the sister group of kinetoplastids. Eukaryot Cell **4**:1137–1146

Maslov DA, Yasuhira S, Simpson L (1999) Phylogenetic affinities of *Diplonema* within the Euglenozoa as inferred from the SSU rRNA gene and partial COI protein sequences. Protist **150**:33–42

Massana R (2011) Eukaryotic picoplankton in surface oceans. Annu Rev Microbiol **65**:91–110

Montegut-Felkner AE, Triemer RE (1994) Phylogeny of *Diplonema ambulator* (Larsen and Patterson): 1. Homologies of the flagellar apparatus. Europ J Protistol **30**:227–237

Montegut-Felkner AE, Triemer RE (1996) Phylogeny of *Diplonema ambulator* (Larsen and Patterson). 2. Homologies of the feeding apparatus. Europ J Protistol **32**:64–76

Moreira D, López-García P, Rodríguez-Valera F (2001) New insights into the phylogenetic position of diplonemids: G + C content bias, differences of evolutionary rate and a new environmental sequence. Int J Syst Evol Microbiol **51**:2211–2219

Moreira S, Valach M, Aoulad-Aissa M, Otto C, Burger G (2016) Novel modes of RNA editing in mitochondria. Nucleic Acids Res **44**:4907–4919

Mylnikov AP (1986) Ultrastructure of a colourless flagellate, *Phyllomitus apiculatus* Skuja 1948 (Kinetoplastida). Arch Protistenkd **132**:1–10

Nguyen L-T, Schmidt HA, von Haeseler A, Minh BQ (2015) IQ-TREE: a fast and effective stochastic algorithm for estimating maximum-likelihood phylogenies. Mol Biol Evol **32**:268–274

Okamoto N, Gawryluk RMR, del Campo J, Strassert JFH, Lukeš J, Richards TA, Worden AZ, Santoro AE, Keeling PJ (2018) *Eupelagonema oceanica* n. gen. & sp. and a revised diplonemid taxonomy. J Eukaryot Microbiol (in press)

Párducz B (1967) Ciliary movement and coordination in ciliates. Int Rev Cytol **21**:91–128

Porter D (1973) I*sonema papillatum* sp. n., a new colorless marine flagellate: a light- and electronmicroscopic study. J Protozool **20**:351–356

Reize IB, Melkonian M (1989) A new way to investigate living flagellated/ciliated cells in the light microscope: immobilization of cells in agarose. Bot Acta **102**:145–151

Roy J, Faktorová D, Benada O, Lukeš J, Burger G (2007) Description of *Rhynchopus euleeides* n. sp. (Diplonemea), a free-living marine euglenozoan. J Eukaryot Microbiol **54**:137–145

Shimodaira H, Hasegawa M (2001) CONSEL: for assessing the confidence of phylogenetic tree selection. Bioinformatics **17**:1246–1247

Scheckenbach F, Hausmann K, Wylezich C, Weitere M, Arndt H (2010) Large-scale patterns in biodiversity of microbial eukaryotes from the abyssal sea floor. Proc Natl Acad Sci USA **107**:115–120

Schnepf E (1994) Light and electron microscopical observations in *Rhynchopus coscinodiscivorus* spec. nov., a colorless, phagotrophic Euglenozoon with concealed flagella). Arch Protistenkd **144**:63–74

Schuster F, Goldstein S, Hershenov B (1968) Ultrastructure of a flagellate, Isonema nigricans nov. gen. nov. sp., from a polluted marine habitat. Protistologica **4**:141–154

Simpson AGB (1997) The identity and composition of the Euglenozoa. Arch Protistenkd **148**:318–328

Skuja H (1948) Taxonomie des Phytoplanktons einiger Seen in Uppland, Schweden. Symb Bot Ups **9**:5–399

Small EB, Marszalek DS (1969) Scanning electron microscopy of fixed, frozen, and dried protozoa. Science **163**:1064–1065

Stamatakis A (2014) RAxML version 8: a tool for phylogenetic analysis and post-analysis of large phylogenies. Bioinformatics **30**:1312–1313

Swale EMF (1973) A study of the colourless flagellate *Rhynchomonas nasuta* (Stokes) Klebs. Biol J Linn Soc **5**:255–264

Triemer RE (1992) Ultrastructure of mitosis in *Diplonema ambulator* Larsen and Patterson (Euglenozoa). Europ J Protistol **28**:398–404

Triemer RE, Farmer MA (1991) An ultrastructural comparison of the mitotic apparatus, feeding apparatus, flagellar apparatus and cytoskeleton in euglenoids and kinetoplastids. Protoplasma **164**:91–104

Triemer RE, Ott DW (1990) Ultrastructure of *Diplonema ambulator* Larsen & Patterson (Euglenozoa) and its relationship to *Isonema*. Europ J Protistol **25**:316–320

Vickerman K (1977) DNA throughout the single mitochondrion of a kinetoplastid flagellate: observations on the ultrastructure of *Cryptobia vaginalis* (Hesse, 1910). J Protozool **24**:221–233

Vickerman K (2000) Diplonemids (Class: Diplonemea Cavalier Smith, 1993). In Lee JJ, Leedale GF, Bradbury P (eds) An Illustrated Guide to the Protozoa **Vol. 2**, 2nd edn, Society of Protozoologists, Lawrence, Kansas, USA, pp 1157–1159

Vlcek C, Marande W, Teijeiro S, Lukeš J, Burger G (2011) Systematically fragmented genes in a multipartite mitochondrial genome. Nucleic Acids Res **39**:979–988

von der Heyden S, Chao EE, Vickerman K, Cavalier-Smith T (2004) Ribosomal RNA phylogeny of bodonid and diplonemid flagellates and the evolution of euglenozoa. J Eukaryot Microbiol **51**:402–416

Yabuki A, Tame A (2015) Phylogeny and reclassification of *Hemistasia phaeocysticola* (Scherffel) Elbrächter & Schnepf, 1996. J Eukaryot Microbiol **62**:426–429

Yurchenko V, Votýpka J, Tesařová M, Klepetková H, Kraeva N, Jirků M, Lukeš J (2014) Ultrastructure and molecular phylogeny of four new species of monoxenous trypanosomatids from flies (Diptera: Brachycera) with redefinition of the genus *Wallaceina*. Folia Parasitol **61**:97–112

Zíková A, Schnaufer A, Dalley RA, Panigrahi AK, Stuart KD (2009) The F0F1-ATP synthase complex contains novel subunits and is essential for procyclic *Trypanosoma brucei*. PLoS Pathog **5**:e1000436, http://dx.doi.org/10.1371/journal.ppat.1000436